International Journal of Applied Chemistry.
ISSN 0973-1792 Volume 19, Number 1 (2023) pp. 1-30

http://www.ripublication.com

Facile Synthesis, Characterization and Screening of Bimetallic Cobalt Complexes for Their Drug Potency

K. R. Swathi[1], M. N. Somashekar[2] and P. R. Chetana[1,3]*

[1]Department of Chemistry, Jnanabharathi Campus, Bangalore University, Bengaluru Karnataka-560056, India
[2]Department of Chemistry, S. S. Margol Degree College, Shahabad, Kalaburagi District, Karnataka-585228, India.
[3]Department of Chemistry, Central College Campus, Bengaluru City University, Bengaluru Karnataka-560001, India
**E-mail: pr.chetana@gmail.com*

Abstract

A new mononuclear, homo binuclear and hetero binuclear complexes with general formulation **[Co (L_1)$_2$]X** (**2**), **[Co (L_1) Co (L)$_2$]X_2** (**3**) and **[Co (L_1) Cu (L)$_2$]X_2** (**4**) where, L_1 is N^1,N^2-bis[3-(dimethylamino) propyl]oxalamide (**1**), L_2 is 1,10-phenanthroline and **X** is ClO_4^-/NO_3^-were synthesized and characterized by UV-Visible, Infrared, NMR, ESI-MS and CHNS elemental analyses. These data are in concordant with molar conductance data which support the evidence for the proposed molecular structures of metal complexes **2**, **3** and **4**. The Time dependant spectra revealed to be stable in the solvent medium which suggests to carryout biological assay in this standard medium. The carcinogenic activity was studied on human cancer cell lines HT-29, HeLa and A549 to evaluate IC_{50} value. Antimicrobial activity was carried on selected bacterial strains *E. coli, S. aureus, E. feacalis, M. luteus, P. aeruginosa* and fungal strains such as *Candida. albicans*, *Aspergillus niger* and *Fusarium oxysporium*. Free radical quenching activity was carried by DPPH, nitric oxide and superoxide dismutase assay. The electronic absorption spectroscopic technique and the gel electrophoresis techniques were evaluated to find the binding efficiency of the mono and bimetal complexes **2**, **3**, and **4** to CT-DNA. The effectiveness of Deoxyribonucleic acid binding studies was examined by using gel documentation system and electronic assimilation spectra.

Keywords: Bimetallic Complexes, Co (II) /Cu (II) complexes, oxamide, DNA Studies, Cytotoxic studies, Antioxidant, Antibacterial assay.

1. Introduction

The fascination of mono and binuclear metal complexes involving N,N′-bis (substituted) oxamides as building blocks owes to their substantial importance in medicinal chemistry. Incorporation of two or more metal centers in a single compound detentions enzyme and cell metabolism to inhibit biological action in a system. Transition metals in their complex state exhibits cytotoxic activities due to properties like charge variation metal ligand interactions, redox activity, partially filled outer orbitals, coordination and bonding, etc., these properties can be attributed to cytotoxic activity of metals. Transition metal complexes have also been found to bind to deoxyribonucleic acid (DNA) in both covalent and non-covalent ways. Metal complexes and DNA interact non-covalently through groove binding, intercalation, and electrostatic interactions [1].

Hetero cyclic base, 1, 10-phenanthroline used as terminal ligand extends aromatic planarity to the complex promotes the DNA non covalent interactions [2-4]. The metal complex with extended planarity plays very important roles in vital cellular functions as well as DNA damage brought on by endogenous oxidation with ageing and cancer induced by proteins containing binuclear metal centres [5-10]. Metal ligand system with strong electronegative groups like oxygen and nitrogen inhibits enzyme metabolism of microorganisms [11-12]. Chelation increases the lipophilic nature of complexes and makes it easier for them to pass through the lipid membranes of the cell wall by curbing the polarity of the metal atom and potentially prompting electron delocalization to result in diminished polarity of the metal ion. This is accomplished by coordinating oxamide-C=O with N donor atoms in heterocyclic bases as well as metal ions [13-14]. When the integrity of a bacterium's cell wall is compromised, it also has an impact on their normal physiology and enzyme metabolism. During chelation, oxygen and nitrogen atoms which are necessary for enzyme activity are rendered inactive. When metal complexes come into contact with a microorganism's cell wall, the integrity of the cell membrane is disrupted and enzyme binding sites are blocked, which slows down the cell's metabolism and prevents the growth of the microorganism.

Entrancing these aspects, the development and synthesis of novel medicinal metal-based antidote with improved non-covalent DNA binding, low toxicity, enhanced selectivity and good chelating ability motivated, our work to synthesise new mono and bimetallic oxamide complexes with 1,10-phenanthroline and evaluate their cytotoxic, antimicrobial and antioxidant potency.

2. Experimental

2.1 Materials and instrumentation

All the chemicals were of AR quality and were utilized precisely as directed. The selected bacterial and fungal strains from the American Type Culture Collection (ATCC) were employed to evaluate the antimicrobial activity of synthesized mono and bimetal complexes. Cancer cell lines procured from the ATCC were used to evaluate the antineoplastic activity of metal complexes. Using a Bruker Ascend 800 MHz NMR instrument, the proton NMR spectra of the synthesized compounds were collected. The FTIR spectra of the synthesized compounds using potassium bromide pellets were

recorded using a Shimadzu spectrophotometer, in the range of 4000 to 400 cm^{-1}. An ESI and APCI probe-equipped Schimadzu-LCMS instrument was used to document mass spectra. UV-Visible spectra were produced using a Systronics 2206, a PC-based dual beam UV spectrophotometer. At the Institution of Excellence in Mysore, elemental studies were carried out availing a Bruker Euro Ea elemental analyzer. The Control Dynamics APX185E conductivity metre with dip type cell and reagent grade 0.1M KCl for calibration was used to measure the molar conductance of the complexes. The melting points were investigated using manual equipment.

2.2 Syntheses

2.2.1 Synthesis of *N, N′-bis[(dimethylpropylenediamine) oxamide];* dmpdox (1)

According to **scheme 1,** in an ice bath, drop by drop, homogeneous ethanol and diethyl oxalate solution (499 mL, 0.1 M, 20 mL) were poured with continual stirring to 3-dimethylamino-1-propyl amine (271 mL, 0.2 M), which had been cooled to 2-3^{o} C. After the completion of addition, approximately five hours were spent heating the reaction mixture in a water condenser at 60 degrees being stirred continuously on a magnetic stirrer. The reaction mixture obtained produced a white colored precipitate after 6 days of gradual evaporation at room temperature [15]. Warm ethanol-water (1:1 v/v) was used to wash the resulting white solid. Recrystallization from ethanol was performed in hot condition and dried over P_2O_5. (**1**)

Anal. Cald. (%) for $C_{12}H_{26}N_4O_2$; (**1**) : C, 55.79; H, 10.14; N, 21.69. Found C, 55.75; H, 10.12; N, 21.45. ^{1}H-NMR (400 MHz, DMSO-d_6, ppm) : δ = 2.17–2.41 (s, 12H), 2.48–2.49 (t, 4H), 3.21–3.25 (t, 4H). FT-IR (KBr disc, cm^{-1}) : ν = 1584 (C=O), 3548 (N-H). λ_{max} (DMF/Tris-HCl) : 238 nm (ε = 1033.39 M^{-1} cm^{-1}). ESI-MS (m/z) : 258.9 [M^+]. Yield: 87.9%. M.P: 82-83 ^{0}C.

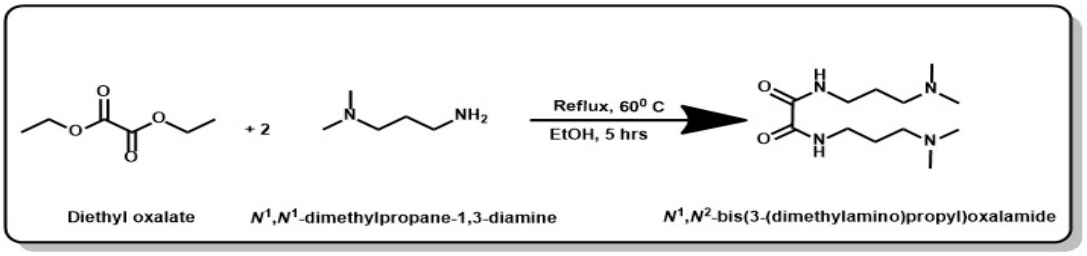

Scheme 1: Propound synthetic path of N, N′-bis[(dimethylpropylenediamine) oxamide] (**1**)

2.2.2 Synthesis of *{μ-trans-N,N′-bis[3-(dimethylamino) propyl]oxamidato} (cobalt (II) tetraoxidochlorate) ;* [Co (dmpdox) $_2$] (ClO_4) (2)

As given in **scheme 2,** drop by drop, dmpdox (**1**) ethanol solution was added to the $CoCl_2.6H_2O$ ethanoic solution (0.1 M, 0.237 g, 10 mL) that had been agitated for three hours. The resultant purple-colored particles were removed through filtration, carefully cleansed with hot ethanol and diethyl ether before being dried at low pressure over P_2O_5 [16]. Recrystallization from ethanol was performed in hot condition and 77.3 percent yield was obtained.

Anal. Cald. (%) for $C_{24}H_{50}ClCoN_8O_8$; (**2**) : C, 42.83; H, 7.49; N, 16.65. Found C, 42.84; H, 7.40; N, 16.68. ^{1}H-NMR (400 MHz, DMSO-d_6, ppm) : δ = 1.72–2.82 (s, 12H), 3.16–3.29 (t, 8H), 8.84–8.87 (m, 2H). FT-IR (KBr disc, cm^{-1}) : ν =1606 (C=O), 3358 (N-H), 551 (M-O), 447 (M-N), 1130; 623 (ClO_4, ionic). λ_{max} (DMF/Tris-HCl) : 230.5 nm (ε = 37359.4 M^{-1} cm^{-1}), 271 nm (ε = 43923.63 M^{-1} cm^{-1}), 524.5 nm (ε = 85010.86 M^{-1} cm^{-1}). ESI-MS (m/z) : 672.3 [M^+] where M = [Co (dmpdox) $_2$]$^{2+}$. Λ_M (DMF, S cm^2 M^{-1}) : 78.34. Yield: 77.3%. M.P: 110-113^{0}C.

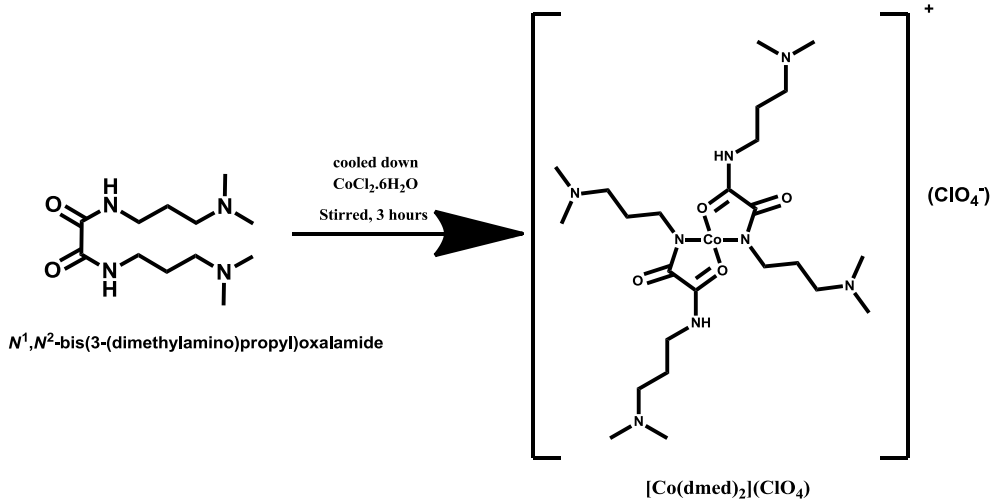

Scheme 2: Propound synthetic path for {μ-trans-N,N′-bis[3 (dimethylamino) propyl) oxamidato} (cobalt (II) tetraoxidochlorate) ; [Co (dmpdox) $_2$] (ClO_4) (**2**)

2.2.3 **Synthesis of *{N,N'-bis (3-(dimethylamino) propyl) oxamidato} (1,10phenanthroline) dicobalt (II) dinitrate;* [Co (dmpdox) Co (phen) $_2$] (NO_3) $_2$ (3)** dmpdox (0.1 mM, 0.515 g, 20 mL) and triethyl amine (0.2 mM, 278 μL, 10 mL) solutions were sequentially added to a Co (NO_3) $_2$.6H_2O (0.095 mM, 0.276 g, 10 mL) solution. The obtained mixture was then swirled at 26^{0}C-27^{0}C (room temperature) for about 30 minutes until it was limpid. After that, contaminants were removed from the reaction mixture by filtering. Under N_2, methanolic solutions of Co (NO_3) $_2$.6H_2O (0.1 mM, 0.291 g, 10 mL) and hetero cyclic base 1,10-phenanthroline (0.2 mM, 0.360 g, 10 mL) to the aforementioned reaction mixture were added drop by drop. A 9-hour reflux process was then performed on the reaction mixture. (**Scheme 3**), the precipitate that resulted was removed, it was thoroughly cleansed with warm methanol and diethyl ether, under decreased pressure and it was dried over P_2O_5 [16]. For recrystallization, a 1:3 mixture of DMF and methanol was utilized.

Anal. Cald. (%) for $C_{36}H_{40}Co_2N_{10}O_8$ (**3**) : C, 50.36; H, 4.70; N, 16.31. Found, C, 50.05; H, 4.46; N, 16.23. ^{1}H-NMR (400 MHz, DMSO-d_6, ppm) : δ = 2.1–2.4 (s, 12H), 3.1–3.2 (s, 2H), 7.5–8.9 (m, 8H). FT-IR (KBr disc, cm^{-1}) : ν = 1645 (C=O), 1521 (C=N), 550 (M-O), 426; 474 (M-N), 1306 (NO_3^-ionic,). λ_{max} (DMF/Tris-HCl) : 212 nm (ε = 21849.55M^{-1} cm^{-1}), 266.5nm (ε = 27401.91 M^{-1} cm^{-1}), 644.5 nm (ε = 75061.44 M^{-1}

cm^{-1}). ESI-MS (m/z) : 421.1 [M+Na+CH_3OH-2 (NO_3^-)] $^+$ where M = M=[Co (dmpdox) Co (phen) $_2$]$^{2+}$. λ_{max} Water/DMF (5%) : Λ_M (DMF, S cm^2 M^{-1}) : 138.25. yield: 69.6%. M.P: 120-123 ^{0}C.

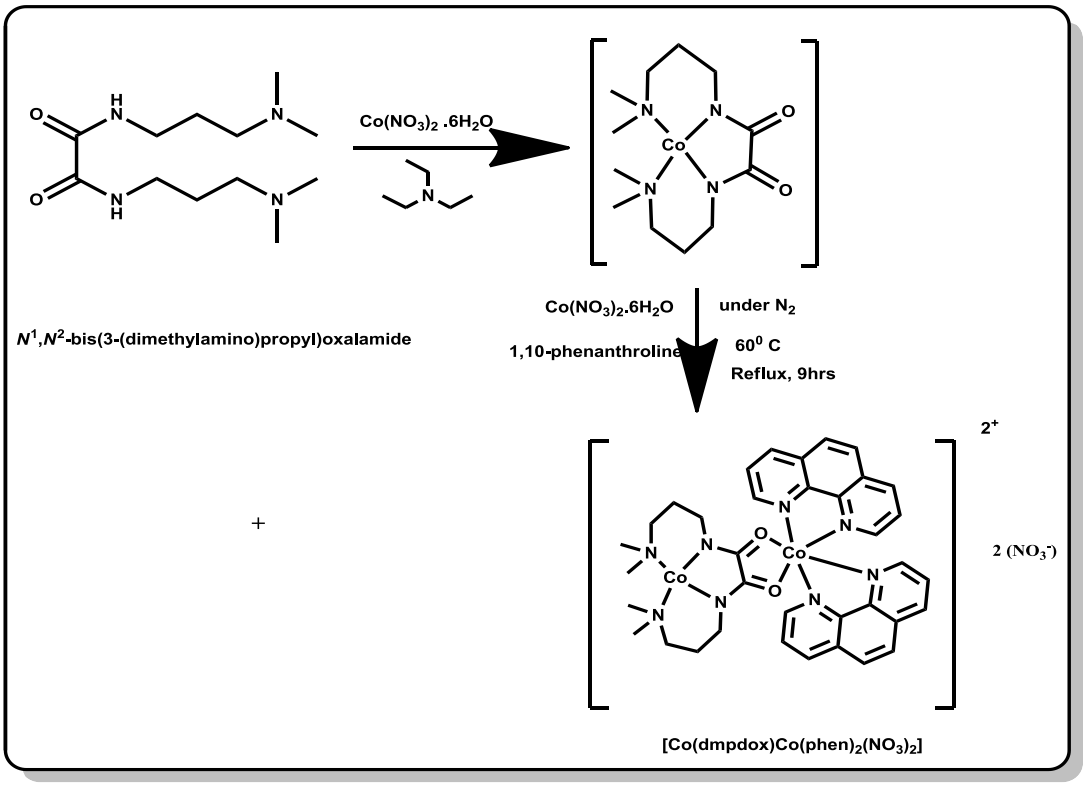

Scheme 3: Propound synthetic path for {N,N′-bis (3-(dimethylamino) propyl) oxamidato} (1,10-phenanthroline) dicobalt (II) dinitrate; [Co (dmpdox) Co (phen) $_2$] (NO_3) $_2$ (**3**)

2.2.4 Synthesis of {*N, N′-bis (3-(dimethylamino) propyl) oxamidato} (1,10-phenanthroline) Cobalt (II) copper (II) dinitrate; [Co (dmpdox) Cu (phen) $_2$] (NO_3) $_2$ (4)*

Cu (NO_3) $_2$.3H_2O (0.095 mM, 0.229 g, 10 mL) and triethyl amine (0.2 mM, 278 µL, 10 mL) methanolic solutions were successively added to a dmpdox (0.1 mM, 0.515 g, 20 mL) solution that was agitated in methanol. The reaction mixture was then filtered to remove impurities after being agitated for approximately 40 minutes at room temperature until it became limpid. Methanolic solutions of Co (NO_3) $_2$.6H_2O (0.1 mM, 0.291g, 10 mL) and 1,10-phenanthroline (0.2 mM, 0.360 g, 10 mL) were added dropwise under N_2 to this reaction mixture. The obtained mixture was next heated constantly at 60^{0}C using reflux condenser for nine hours (**Scheme 4**), the precipitate that resulted was then filtered out, it was thoroughly cleansed with warm methanol followed by diethyl ether, under decreased pressure the product was dried over P_2O_5 [16]. DMF/methanol (1:3) was used to Recrystallization.

Anal. Cald. (%) for $C_{36}H_{40}CoCuN_{10}O_8$ (**4**) : C, 50.09; H, 4.67; N, 16.23. Found, C, 50.32; H, 4.49; N, 16.22. ^{1}H-NMR (400 MHz, DMSO-d_6, ppm) : δ = 2.2 – 2.8 (s, 2H), 2.9 – 3.0 (s, 2H), 7.4 – 8.9 (m, 8H). FT-IR (KBr disc, cm^{-1}) : ν = 1627 (C=O), 1519 (C=N), 559 (M-O), 421; 493 (M-N), 1323 (NO_3^-ionic,). λ_{max} Water/DMF (5%) : 247 nm (ε = 29574. M^{-1} cm^{-1}), 296.5 nm (ε = 35500.9 M^{-1} cm^{-1}), 634.5 nm (ε = 108651.1 M^{-1} cm^{-1}) ESI-MS (m/z) : 369.6 [M^+-2 (NO_3^-)] $^+$ where M=[Co (dmpdox) Cu (phen) $_2$]$^{2+}$. Λ_M (DMF, S cm^2 M^{-1}) : 155.32. yield: 712%. M.P: 126-127 ^{0}C.

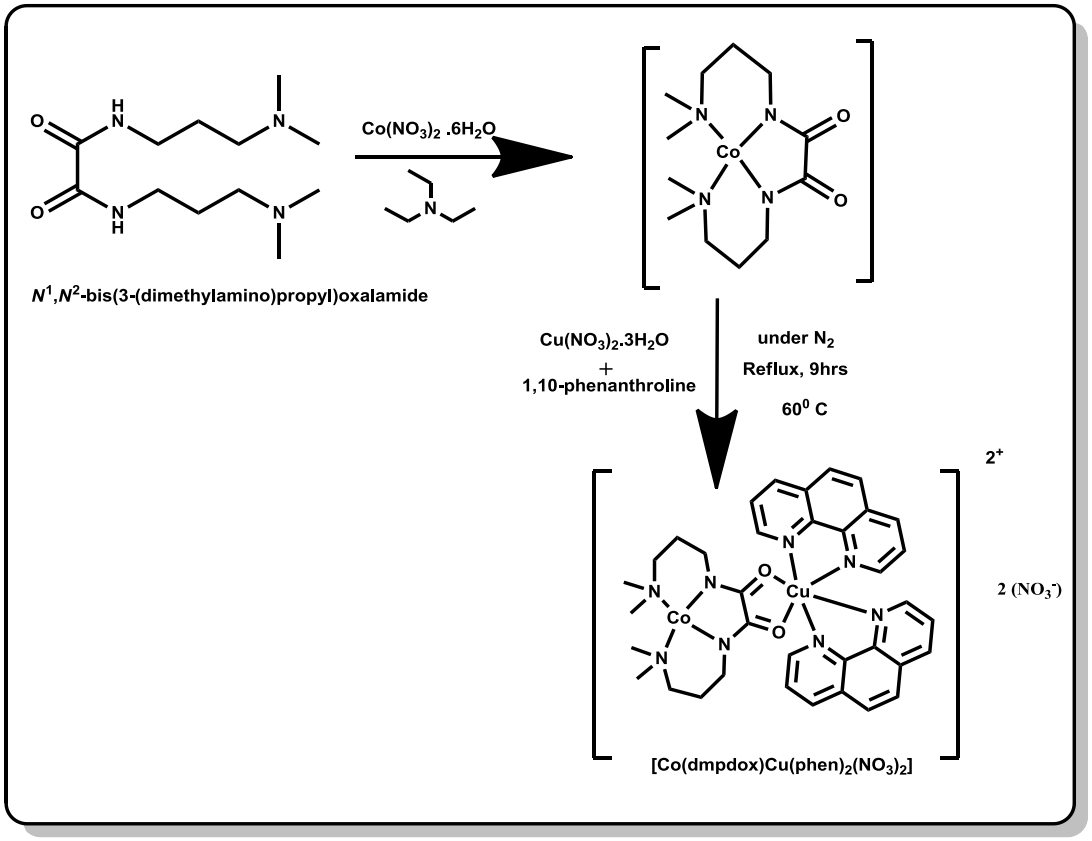

Scheme 4: Propound synthetic path for {N,N′-bis (3-(dimethylamino) propyl) oxamidato} (1,10-phenanthroline) dicobalt (II) dinitrate; [Co (dmpdox) Cu (phen) $_2$] $(NO_3)_2$ (**4**)

2.3 Deoxyribonucleic acid binding studies

2.3.1 Investigations of binding efficacy of DNA by UV-Visible absorption method

Using Calf thymus, electronic absorption tests were conducted to test the DNA binding ability of monometal **2**; homogeneous bimetal **3**; and heterogeneous bimetal **4** complexes. The concentration of Calf thymus DNA was increased by 2.5 µM aliquots up to 10 µM during the experiments. To obliterate absorption caused by free CT-DNA, in reference compartment an equimolar amount of CT-DNA was mixed with a pure buffer solution to attribute spectra with metal complexes. The comparatively small shift

in absorption intensity in response to DNA concentration was used to construct titration curves. The intrinsic binding constant was computed using titration curve analysis (K_b). The linear fit curve was plotted in Origin software to assess the binding constant of metal complexes (version 6.1). By measuring UV-Visible absorbance and recording incremental DNA addition by following equation **(a),** binding constant of mono and bimetal complexes are calculated. [17–18].

$$[DNA]/(\varepsilon_a-\varepsilon_f) = [DNA]/(\varepsilon_b-\varepsilon_f) + 1/K_b(\varepsilon_b-\varepsilon_f) \quad \textbf{(a)}$$

In the aforementioned equation, the extinction coefficients ε_a (for every additament of CT-DNA to the metal complex), ε_f (the complex without DNA; as determined by Beer's law from the calibration curve of the relevant metal complex) and ε_b (the complex when fully bound to DNA)

2.3.2 Deoxyribonucleic acid binding studies by gel electrophoresis method

The complexation coherence of a DNA mixture was evaluated with the aid of gel electrophoresis and EtBr intercalation appraisal. Following an hour of incubation at room temperature, the prepared mixtures were infused onto the gel at a concentration of 100 ng/well using gel loading TAE buffer. Thereafter, 45 minutes of electrophoresis in 1 TAE buffer at 5 Vcm^{-1} were carried out. UV Trans illumination on the Chemi Doc Bio rad was used to see how free DNA migrated on the gel. Using naked DNA bands as a standard, the amount of free DNA was measured, and band densities were calculated using the Image J1.50c programme. The following expression was used to calculate the complexation coherence:

$$\text{Complexation coherence (\%)} = (BD_{Std}\,DNA - BD\ sample) \times 100/BD_{Std}\,DNA$$

Where BD_{std} DNA and BD sample stand for band densities with standard (free DNA or unbound DNA) and band densities of parent ligand dmpdox (**1**) and its corresponding metal complexes **2**, **3** and **4.** where band intensity gives the abundance of CT-DNA present after complexation with metal complexes [19-20].

2.4 Free radical scavenging activities of metal complexes

2.4.1 DPPH Radical Scavenging

Antioxidants converts purple colored DPPH into the colorless molecule. 1,1-diphenyl-2-picryl hydrazine, which is measured at an absorbance of 590 nm. DPPH scavenging assay for the ligand **1** and its mononuclear and binuclear complexes **2**, **3** and **4** were found by amending the reported technique [21]. One milligram of prototype samples was mixed to create stock solutions for testing (mononuclear and binuclear complexes **2**, **3** and **4**), in 1 mL DMSO. Different test solution concentration was taken in a 96-well plate by twofold dilution. HPLC grade methanol was used to make volumes up to 240 µL, and 80 µL of DPPH was introduced to all the wells. Since DPPH is photosensitizer, immediate 15-minute incubation in the dark at 25°C was performed on the reaction mixture. A blank solution without the test sample was carried out along with standard quercetin. Both the standard and blank solution wells were prepared using

same protocol as of test samples. Then, using a semi-autoanalyzer, absorbance was determined at 590 nm. Comparative studies of the metal complexes and the antioxidant quercetin were conducted. IC_{50} values and percent inhibition are calculated using nonlinear regression analysis, which is done for various test sample concentrations and reference samples. Percent of impediment was recorded for reference and different sample concentrations by nonlinear regression analysis by making use of Graph Pad Prism software version 6.0. The IC_{50} value is not calculated for samples that have inhibition levels below 50%. By contrasting the sample's IC_{50} value with the standard, the sample's relative activity was assessed. The relative activity will be lower in relation to the standard if the IC_{50} value is higher, and vice versa. The complex's capacity to scavenge DPPH radicals was assessed using a drop in absorbance, which determines the amount of metal complexes needed to effectively scavenge 50% of DPPH radicals.

2.4.2 Nitric oxide scavenging assay

By modifying the previously published procedure [22], the nitric oxide scavenging assay for the ligand **1** and its mononuclear and binuclear complexes **2, 3** and **4** were determined. The diazotization reaction is the basis for the nitric oxide assay. In an acidic environment (phosphoric acid), sulfanilamide and N-1-napthylethylenediamine have the ability to identify NO_2 in cellular matrices like serum, plasma etc., Stock solutions for test samples were made by dissolving one milligram of the test substances in one milliliter of DMSO.1 mL of a 1 mM nitrite standard (curcumin) was prepared in the pH 7.0 phosphate saline buffer (8 g of NaCl, 1.21g of K_2HPO_4 and 0.34g of KH_2PO_4 in 1000 mL distilled water.) For the experimental samples, 50 μL of the stock solution (160, 80, 40, 20, 100 μM) and standard (1000, 500, 250, 125, 6.25 and 31.3 μM) were added to the 96-well plate by twofold dilution concentration using a multichannel pipette. Buffer was added to the last set of well with no test sample solutions. Each well's final volume was 50 μL and the nitrite concentration range was 0-1000 mM and then 50 μL of Griess reagent (1 g 4-amino benzene sulfonamide dissolved in five percent H_3PO_4 solution in de-ionized water and 10 mg of 0.1% N–napthyl ethylene diamine dissolved in 10 mL de-ionized water, was mixed in 1:1 ratio just before using the reagent) was added to all experimental sample wells. It was left to stand at room temperature for 10 minutes. At 546 nm plate reader was used to assess the absorbance. A blank solution without the test sample was carried out along with standard curcumin. Both the standard and blank solution wells were prepared using same protocol as of test samples. Graph Pad Prism 6 was operated to compute the nitrite concentration from a variable and sigmoid dose response curve, a nonlinear regression analysis (curve fit) was produced to derive IC_{50} values.

2.4.3 SOD enzyme catalysis

SOD enzyme catalyses the reformation of potentially toxic superoxide to less toxic hydrogen peroxide and molecular oxygen by redox reaction. Metal ion reduction and superoxide ion oxidation occur simultaneously in this process. Samples tested for super oxide dismutase assay has showed the potency to quench superoxide. Water dispersible salt WST-1 [2-(4-Iodophenyl)-3-(4-nitrophenyl)-5-(2,4-disulfophenyl)-2H-tetrazolium, monosodium salt] that was used in the SOD Determination Kit (19160

SOD, Sigma Aldrich purchase), which leads to the formation of formazan dye that is water-soluble when reduced with O_2^-. At 450 nm, by measuring a reduction in color development, which is inversely correlated to the activity of xanthine oxidase (XO) and rate of oxygen reduction inhibited by SOD, it is feasible to assess the SOD activity as an inhibitory activity [23–24]. Sample well and blank well were loaded with 200 µL working solution (WS) and 20 µL enzyme working solution (EWS). In a 96-well microplate previously loaded with 20 µL of the sample and double-distilled water, incubated for about 20 minutes at 37 °C. With the aid of an optical microplate reader, the absorbance at 450 nm was recorded. The following formula was used to calculate the SOD inhibitory activity. With the aid of Graph Pad Prism 6, using a variable and sigmoid dose response curve, a nonlinear regression analysis (curve fit) was produced to derive IC_{50} values. The inhibition rate and SOD activity were computed using the equation below:

$$SOD\ activity\ (inhibition\ rate\ \%) = \frac{Absorbance\ (control) - Absorbance\ (test\ sample)}{Absorbance\ (control).} * 100$$

$$SOD\ \frac{mU}{mL} = \frac{SOD\ (nM)}{Absorbance * Reaction\ volume(ml)} * 2$$

2.4 Cytotoxic activities

Counting live cells after staining with the essential dye MTT has been used to identify the negative in vitro effects of metal complexes. (3-[4, 5-dimethylthiazol-2-yl]-2, 5-diphenyl tetrazolium bromide) when made in a medium or salt solutions devoid of phenol red, the water-soluble tetrazolium salt used in the MTT method, which uses mitochondrial dehydrogenases to gauge the activity of viable cells by yielding a yellowish solution. The dissolved MTT's tetrazolium ring was broken down by the enzyme mitochondrial dehydrogenase of viable cells to create an insoluble purple formazan. To solubilize water-insoluble formazan formed, DMSO was utilized. A spectrophotometric analysis of the resultant purple solution is performed. The amount of formazan produced changes in tandem with a change in cell number, showing the degree of viable cells following MTT dye staining has been employed to assess the harmful effects of metal complexes in vitro [25–26]. A spectrophotometric analysis of the resultant purple solution is performed. The degree of inhibition of the cytotoxic effects of metal complexes can be measured by the rate of formazan production, which is directly proportional to the number of cells present. Stock cells (cancer cells) from the ATCC were cultured in DMEM/RPMI until confluent. Using a cell-dissociating solute ion [(0.2 percent trypsin ($C_{35}H_{47}N_7O_{10}$), 0.02 percent ($C_{10}H_{16}N_2O_8$) ethylene diamine tetracetic acid, 0.05 percent glucose ($C_6H_{12}O_6$) in phosphate buffered saline (PBS)] the cells were broken up after examining cell's vitality they were centrifuged. Additionally, a 96-well plate with 50,000 Each well was seeded with cells, and they were then allowed to proliferate for 24 hours at 37 ^oC and 5 percent CO_2. The published method was modified for the MTT assay for the metal complexes [27-29].

DMSO was used to dissolve the formazan that had formed, after the supernatant was drained from the plates. An absorbance measurement was made using a microplate reader and a 590 nm wavelength. [30–32]. The test drug concentrations required to arrest growth of cells by 50% (IC_{50}) were calculated using the percent inhibition formula and were based a variable and sigmoid dose response curve, a nonlinear regression analysis produced with the aid of Graph Pad Prism 6.

2.6 Antimicrobial activities:

The potency of the synthesized mononuclear, homo binuclear and hetero binuclear metal complexes along with its parent ligand dmpdox was tested for a few types of fungi and bacteria by using a conventional disc diffusion method on nutrient agar slants by modifying reported method [33-34]. E. coli, S. aureus, E. feacalis, M. luteus, and P. aeruginosa were inoculated using peptone broth, and the injections were inoculated for 30 hours at 37 °C. While potato dextrose agar was prepared and inoculated with C. albicans, A. niger, and F. oxysporium cell suspensions, cultures were then rested for 48 hours at 27°C and were adjusted to 1-2x 10^5cells/ml. Inoculated Soyabean Casein Digested agar plates and Potato Dextrose agar plates (90 mm) are added with ciprofloxacin and itracanazole (25µl) respectively and a Control (25µl) was added to the agar plates. standard antibiotic ciproflaxin and one test sample (50 g mL^{-1} and 100 g mL^{-1} were added in each test plate for bacterial strains while standard itracanazole and one test sample were added to each test plate for fungal strains. All discs were inoculated with DMSO as negative control. According to the molecular weight 10Mm solution of metal complexes **2**, **3** and **4** along with their parent ligand **1** were prepared and were added to test plate. The treated plates were inoculated at 37^0C and 27^0C for bacterial (24 hrs) and fungal strains (48 hrs) respectively. After incubation, the petri dish was checked for an inhibition zone. The minimum inhibitory concentration (MIC) for metal complexes that have shown inhibitory activity is calculated by operating Graph Pad Prism 6 to analyse a nonlinear regression by variable and sigmoid dose response curve. Obtained data are fitted using a series of approximations. Dose response curve was prepared by using ciproflaxin and itracanazole for bacterial and fungal strains respectively which are used as positive control in agar well diffusion study for the respective strains.

3. Results and discussions

3.1 IR spectroscopy

IR spectrum (Figure 1) of the free ligand dmpdox respectively shows carboxyl and amide stretching vibrational bands in the ranges of 1584 cm^{-1} and 1606 cm^{-1} [35]. In mononuclear metal complex **2** bathochromic shift in carbonyl group and hypsochromic shift in amide group [36] is unveiled which is 1606 cm^{-1} and 3358 cm^{-1} along with 551 cm^{-1} and 447 cm^{-1} bending frequencies are associated for metal to oxyl and amide binding respectively [37] also distinctive signals at 1130 cm^{-1} and 623 cm^{-1} are the evidences for the existance of non-coordinated perchlorate group [38]. In complex **3** and complex **4**, bending vibrations remarked in the range 421-488 cm^{-1} and 551-559 cm^{-1} are respectively associated for ν (M-O) and ν (M-N) bonding. ν (N-H) stretching

mode and C=O deformation peak at 718 cm^{-1} present in parent ligand dmpdox has disappeared and is accompanied by 1533 cm^{-1} and 1519 cm^{-1} bands which denotes the binding of 1,10-phenanthroline as terminal ligand to the complexes **3** and **4** respectively [9-11]. ν (C=O) vibration bands of metal complexes **3** and **4** are remained around the ν (C=O) of dmpdox this is due to the following reasons, deprotonated amide nitrogen and metal ion coordinates to form mono nuclear metal complex. The amide I band displaces significantly toward the greater or lesser wave number and amide I band degenerates and moves back to its initial position when the bridging ligand for two metal ions is oxamide dianion. In comparison to the corresponding mononuclear metal complexes, the C=O binuclear complexes have a higher bond order. Generally, in binuclear complexes this dislocation in shift confirms oxamido bridge, in addition to that presence of ionic nitrate group has indicated by significant peaks at 1306 cm^{-1} and 1323 cm^{-1} in bimetal complex **3** and **4** which further provides proof for the existence of coordinated nitrate ion in hetero binuclear complexes. These spectral data (**Table 1**) are in concordant with NMR spectra and molar conductance data which support the evidence for the proposed molecular structures of metal complexes **2**, **3** and **4**.

Table 1: IR Spectral data for **1**, and its mononuclear **2,** hetero binuclear **3** and **4** metal complexes

Compound IR (Cm^{-1})							
Code	**υ (C=O)**	**υ (N-H)**	**υ (C=N)**	**υ (M-O)**	**υ (M-N)**	**(ClO_4^-)**	**υ (NO_3^-) (ionic)**
1	1584	3548	-	-	-	-	-
2	1606	3358	-	551	447	1130, 623	-
3	1645	-	1521	550	426, 474	-	1306
4	1627	-	1519	559	421, 493	-	1323

Note: **(1)** = Dmpdox, **(2)** = [Co (dmpdox) $_2$] (ClO_4), **(3)** = [Co (dmpdox) Co (phen) $_2$] (NO_3) $_2$ and **(4)** = [Co (dmpdox) Cu (phen) $_2$] (NO_3) $_2$

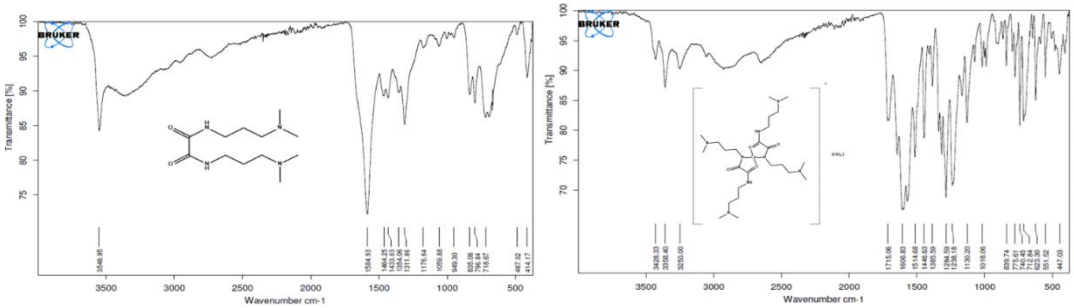

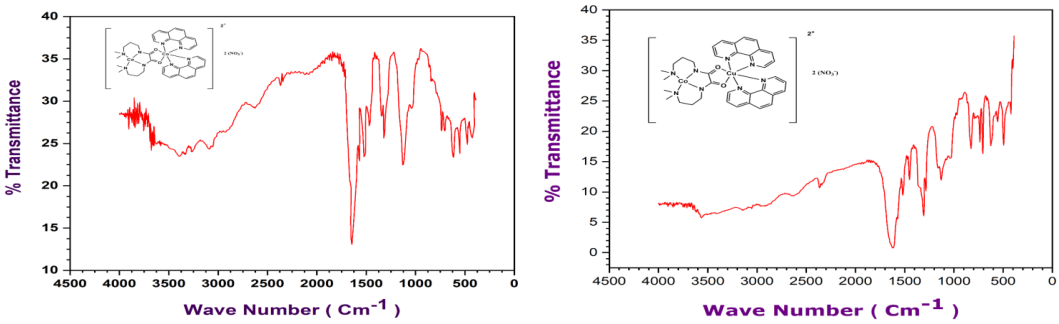

Figure 1: IR spectrum of dmpdox (**1**) and its complexes [Co (dmpdox) $_2$] (ClO_4), (**2**), [Co (dmpdox) Co (phen) $_2$] $(NO_3)_2$ (**3**) and [Co (dmpdox) Cu (phen) $_2$] $(NO_3)_2$ (**4**) in KBr disc.

3.2 ^{1}H NMR spectroscopy:

^{1}H NMR spectra (**Figure 2**) of **1**, **2**, **3** and **4** exhibit δ values in the region 2.3-3.2 ppm for alkyl –CH_2 protons [39], chemical shift values falling in the range 8.84 to 8.87 ppm corresponds to amide –NH protons, chemical shift values in the range 7.4 to 8.9 ppm corresponds to aromatic protons of hetero cyclic base of 1,10-phenanthroline [40]. Complex **2** exhibits δ values in the range 1.7 to 2.8 ppm and 8.84 to 8.87 ppm attributes to alkyl –CH_2 protons and –NH protons respectively. Appearance of δ value corresponding to –NH protons remarks the participation of amide –NH protons in complexation of mononuclear complex **2** [41]. Complex **3** has chemical shift values of alkyl –CH_2 and aromatic protons of 1,10-phenanthroline at 2.1-2.4 ppm and 7.5-8.9 ppm respectively. ^{1}H-NMR spectra revealed the absence of amide –NH protons with respect to mononuclear complex **2**, evidences for coordination of amide –NH protons with metal ion and presence of aromatic protons of heterocyclic base, confirms the formation of binuclear complex **2** by deprotonation of amide –NH protons [42].

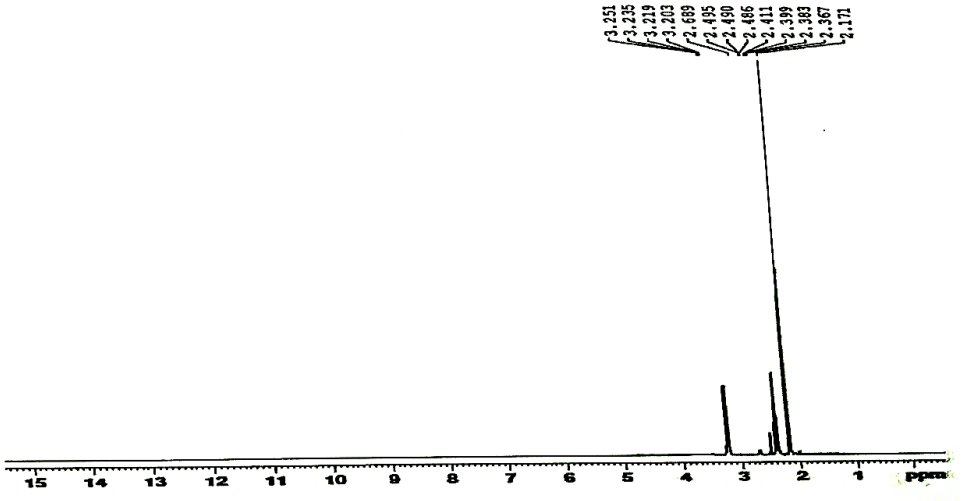

Figure 2.0: ^{1}H-NMR spectrum of ligand (**1**) dmpdox in DMSO-d_6 using TMS as standard.

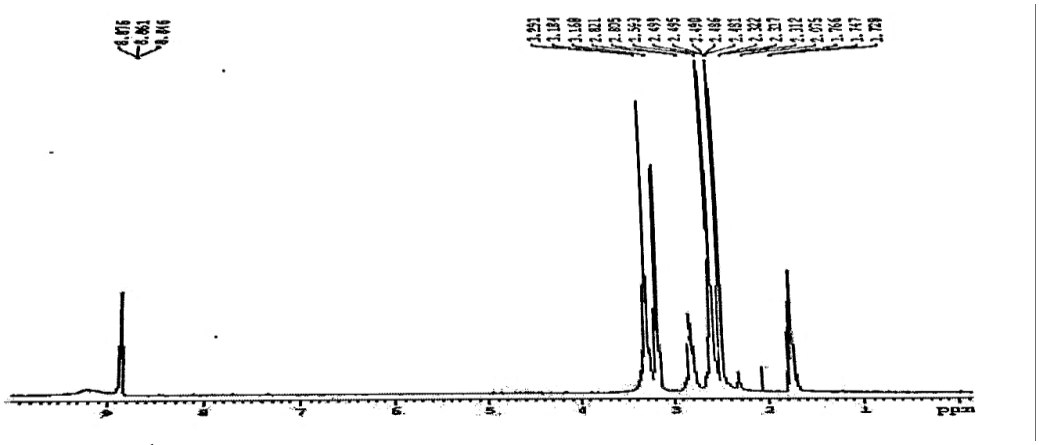

Figure 2.1: ^{1}H-NMR spectrum of [Co (dmpdox) $_2$] (ClO_4), (**2**), in DMSO-d_6 using TMS as standard.

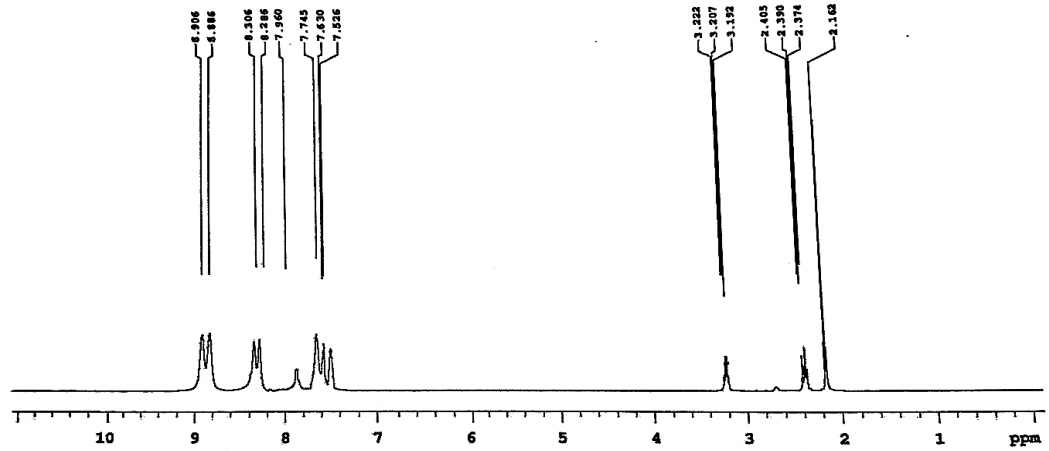

Figure 2.2: ^{1}H-NMR spectrum of [Co (dmpdox) Co (phen) $_2$] (NO_3) $_2$ (**3**) in DMSO-d_6 using TMS as standard.

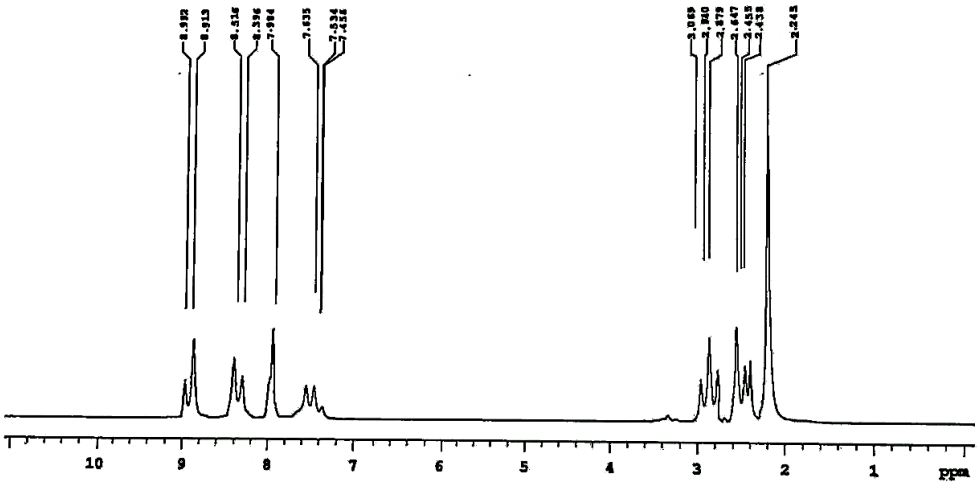

Figure 2.3: ^{1}H-NMR spectrum of [Co (dmpdox) Cu (phen) $_2$] (NO_3) $_2$ (**4**) in DMSO-d_6 using TMS as standard.

3.3 Ultra violet and visible spectroscopy

Table 2 displays the electronic spectral data of ligand dmpdox and its respective mono and binuclear complexes are shown in **Table 2**. A sharp peak at 230 nm was observed in the ligand dmpdox **1** that might have been caused by intra-ligand charge transfer. The charge transfer absorption band has short wavelength ranges because of the interaction between the spin exchange between the metal ions and the π-path orbital generated by the oxamido bridge All three metal complexes exhibit absorption bands of varying intensities; intense peaks seen between 212.5 nm and 290 nm are ascribed to ligand to metal (LMCT) or metal to ligand charge (MLCT) transitions, respectively. Low intensity broad bands obtained in the region of 644.5 nm to 524 nm may be associated to d-d transitions [43], decrease in the frequency of d-d transition in binuclear complex with respect to mononuclear complex may be noticed, this decrease constitutes due to the reduction in the planarity of the metal oxamide chromophore [MN_4] when the binuclear complex is formed with the second metal during the bimetallic complexation [44]. We noticed a broad d-d band that was unresolvable even though the two metal ions are present in two distinct co-ordination sites [45]. Further support for the complexes proposed structures are given by IR, ESI-MS, NMR and molar conductance studies.

Table 2: Electronic spectral data of dmpdox **1** and its mononuclear **2,** hetero binuclear **3** and **4** metal complexes

UV (nm)	λ_{max}/nm (ε/$dm^{-3}m^{-1}cm^{-1}$)		
Sl. no.	Sample	d-d	CT
1	Dmpdox (**1**)	-	238.0 (1033)
2	[Co (dmpdox) $_2$] (ClO_4) (**2**)	524 (850)	230.5 (373), 271.0 (439)
3	[Co (dmpdox) Co (phen) $_2$] (NO_3) $_2$ (**3**)	644.5 (750)	212.5 (218), 266.5 (274)
4	[Co (dmpdox) Cu (phen) $_2$] (NO_3) $_2$ (**4**)	634 (759)	247.0 (295), 296.5 (355)

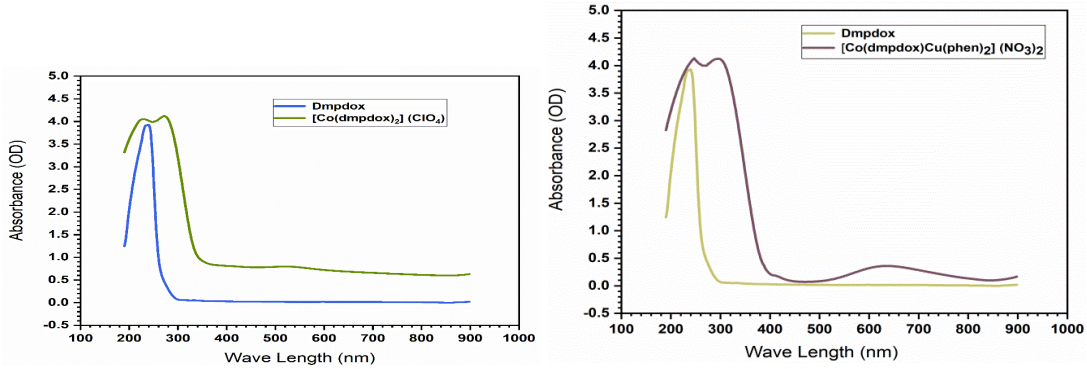

Figure 3: UV-Visible absorption spectra of ligand dmpdox (**1**) and [Co (dmpdox) Cu (phen) $_2$] (NO_3) $_2$ (**4**) in 10^{-3} M solutions DMSO and H_2O (V_{DMSO}: V_{water} = 1:9).

Time dependent stability study of all the three complexes were conducted in solvent medium DMSO/DMF and H_2O ($V_{DMSO/DMF}$: V_{H2O} = 1:9). All the complexes are

revealed to be stable in this solvent medium which suggests to carry out biological assay in this standard medium (**Figure 4**).

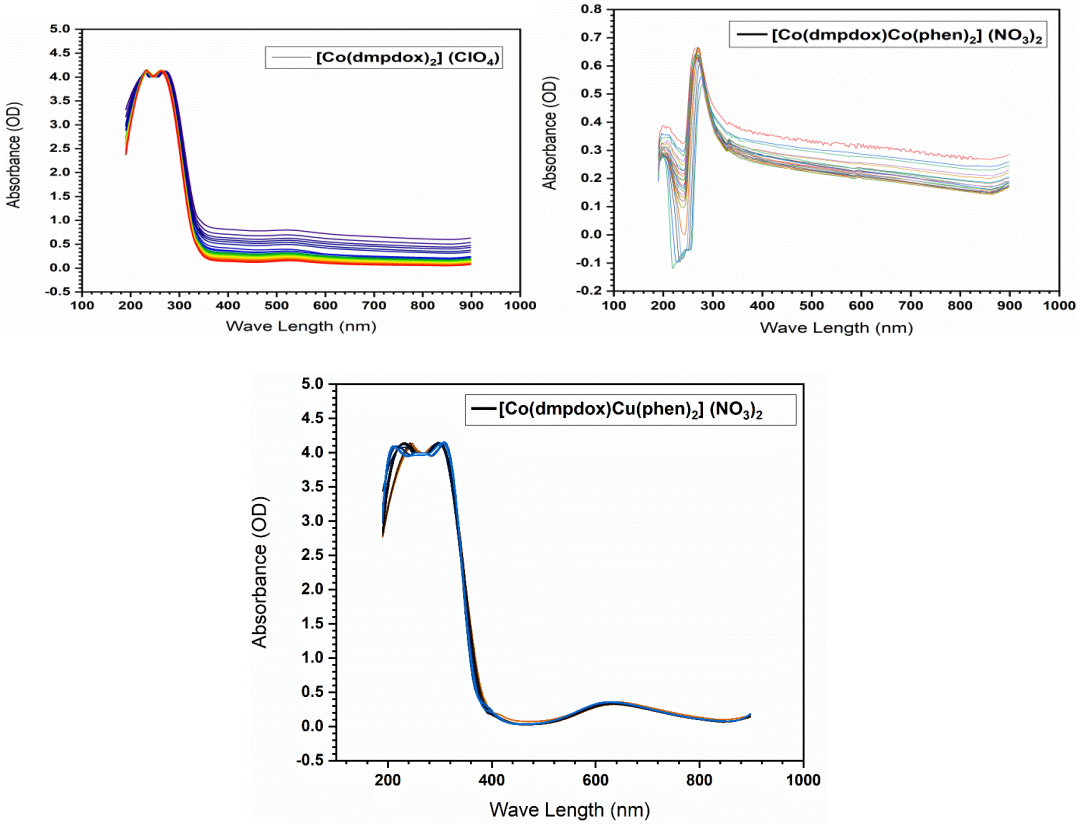

Figure 4: Time dependent stability study of complexes [Co (dmpdox) $_2$] (ClO_4), (**2**), [Co (dmpdox) Co (phen) $_2$] (NO_3) $_2$ (**3**) and [Co (dmpdox) Cu (phen) $_2$] (NO_3) $_2$ (**4**) by UV-Visible absorption spectroscopy over 6h in DMSO and H_2O (V_{DMSO}: V $_{water}$ = 1:9).

3.4 ESI-MS spectroscopy

ESI-MS spectra (Figure 5) confirm the formation of the ionic complexes and ligand. The m/z peak recorded in positive ion mode for **1**, **2, 3** and **4** is in accordance with $[M]^+$=258.9 a.m.u and $[M^+]$ = 672.3 a.m.u, $[M+Na+CH_3OH-2\ (NO_3^-)\ ]^+$ = 406.4 a.m.u and $[M^+-2\ (NO3^-)\ ]^+$= 368.7 a.m.u respectively depending on the experimental conditions positively charged ions like H^+, Na^+, K^+ or solvent molecule interferes in ESI-MS mode. The ESI-MS spectra recorded in methanol for ligands and their respective complexes confirms the formation of ligands and ionic complexes noting that depending on the apparatus and experimental conditions, additional positively charged species such as H+, Na+, K+, solvent molecules, etc. interact with ESI-MS spectra in positive scan mode and may appear as background ions with the m/z peak [46-47]. Sample **1** has shown base peak value at 258.9 a.m.u corresponding to M^+ peak this confirms the formation of ligand **1**. Sample **2** has shown base peak value at 672.3 a.m.u. corresponding to M^+ peak this confirms the formation of [Co (dmpdox) $_2$] (ClO_4)

(**2**). In complex **3**, the base peak m/z value 421.1 a.m.u. which is in accordance with [M+Na+CH_3OH-2 (NO_3^-)]$^+$ ion peak where M=[Co (dmpdox) Co (phen) $_2$]$^{2+}$ ion which indicates the formation of [Co (dmpdox) Co (phen) $_2$] (NO_3) $_2$ (**3**). The mass spectra of complex **4** has m/z value 369.6 a.m.u. which is in accordance with [M^+-2 (NO_3^-)]$^+$ ion peak where M=[Co (dmpdox) Cu (phen) $_2$]$^{2+}$ ion indicates formation of [Co (dmpdox) Cu (phen) $_2$] (NO_3) $_2$ (**4**) m/z values of mass spectra of **1**, **2**, **3** and **4** which are in compatible with FTIR, NMR, spectra along with molar conductance values and CHNS analysis, formation of complexes can be concluded. Spectral results are correlated with respective synthesized ligands and complexes. The spectral data are within the predicted range and are associated with the corresponding compounds and complexes. As determined by molar conductance studies in the DMF solvent, complexes **3** and **4** are 1:2 electrolytes and complex **2** is a 1:1 electrolyte.

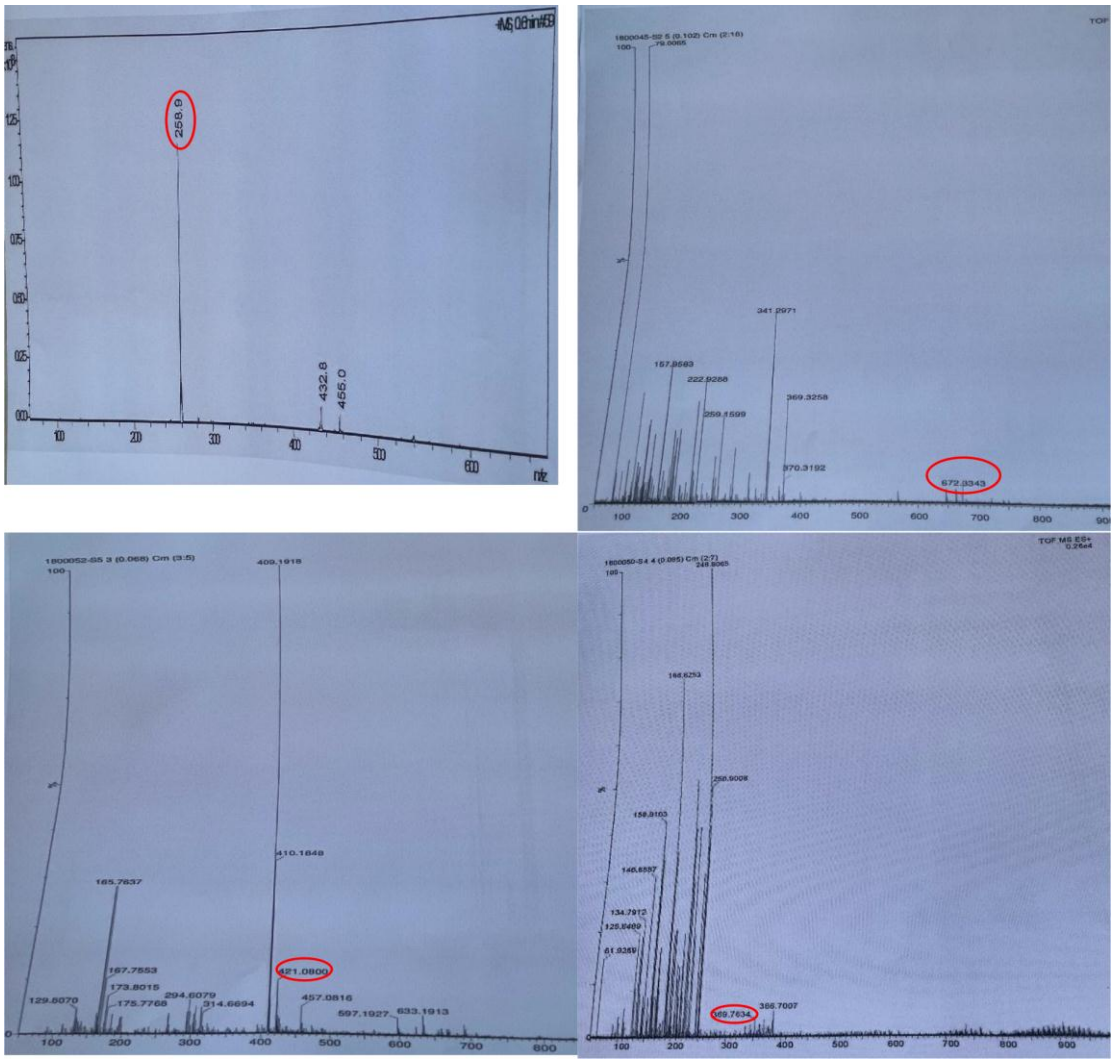

Figure 5: ESI-Mass spectrum of ligand dmpdox (**1**) and its complexes [Co (dmpdox) $_2$] (ClO_4), (**2**), [Co (dmpdox) Co (phen) $_2$] (NO_3) $_2$ (**3**) and [Co (dmpdox) Cu (phen) $_2$] (NO_3) $_2$ (**4**) in positive ion mode in CH_3OH

3.5 Calf thymus-Deoxyribonucleic acid binding studies

3.5.1 Deoxyribonucleic acid binding studies by Ultra Violet-Visible absorption Masss spectra resolution change method:

Absorption titration curves were constructed by UV-Visible absorption titration technique for metal complexes **2**, **3**, and **4** using origin version 6**.** Titration curves were constructed for complex without DNA (ε_f) and the complex when fully bound to DNA (ε_b). A_{obs}/[complex] was used to calculate ε_a The following equation was used to fit the data, where, y-intercept is $1/[K_b (\varepsilon_b - \varepsilon_f)]$ and $1/(\varepsilon_b - \varepsilon_f)$ is slope. K_b was calculated by dividing slope by intercept.

Plots comparing *[DNA]/* $(\varepsilon_a - \varepsilon_f)$ and [DNA], were used to estimate binding constants which were found to be 2.43 x 10^3 M^{-1} (r = 0.9099) (**2**), 2.77 x 10^3 M^{-1} (r = 0.8663) (**3**) and 2.70 x 10^3 M^{-1} (r = 0.9886) (**4**) (**Table 3**) in the order: **2**> **4** > **3**. **Figure 6-8** demonstrates how the quantity of CT-DNA in the metal complexes alters absorption intensities spectral bands in relation to the linear fit curve response. The distinctive spectrum alteration in Complex **2** is exhibiting hyperchromism which indicates Complex **2** is bound to DNA either by electrostatic interaction mode or by groove binding interaction mode. Expanded planar phenanthroline bases in complexes **3** and **4** encourage non-covalent interactions between the complexes and DNA. [48-49]. The distinctive spectrum alterations in intercalative mode are exhibiting hypochromism and a very slight bathochromic shift (~4 nm). This may be brought on by a repercussion between the DNA base pairs' π-orbitals and the π*-orbitals of intercalated complexes, which lowers the π-π * bathochromic shift induced by transition energy. Additionally, electrons in the π-π* orbital are partially filled as a result of coupling, which lowers transition probabilities and induces hypochromism.

Table 3: Specification of K_b for Metal Complexes **2**, **3**, and **4**

Sl No.	Compound EmpiricalIntrinsic formula	K_b (M^{-1})
1	[Co (dmpdox) $_2$] (ClO_4) (**2**)	2.43 x 10^3
2	[Co (dmpdox) Co (phen) $_2$] (NO_3) $_2$ (**3**)	2.77 x 10^3
3	[Co (dmpdox) Cu (phen) $_2$ (NO_3)] (NO_3) $_2$ (**4**)	2.70 x 10^3

K_b = Intrinsic binding constant (M^{-1}).

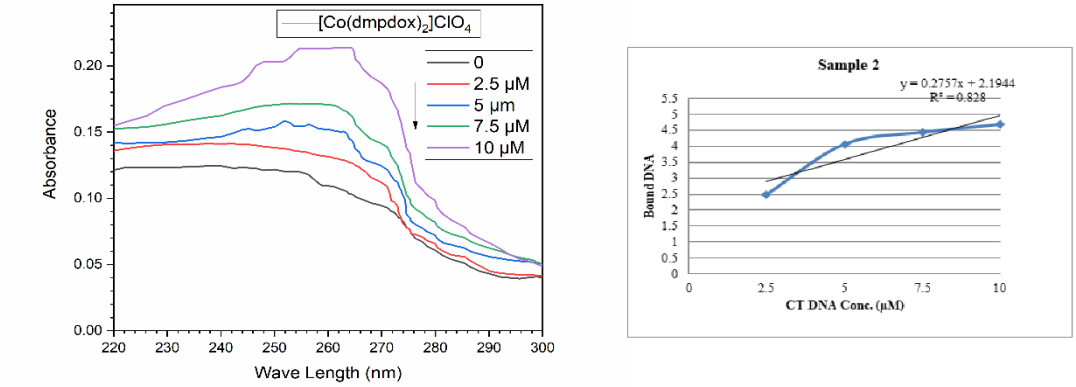

Fig 6: Titration curves of complex **2 by** UV-Visible absorption spectroscopy; buffered (pH = 7.2) at 25 ˚C representing free and fully bound complex.

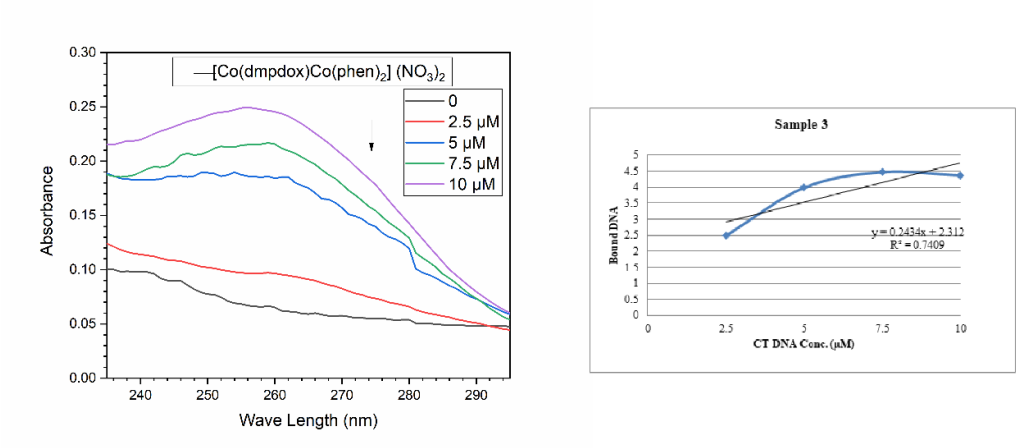

Fig 7: Titration curves of complex **3** by UV-Visible absorption spectroscopy; buffered (pH = 7.2) at 25 ˚C representing free and fully bound complex.

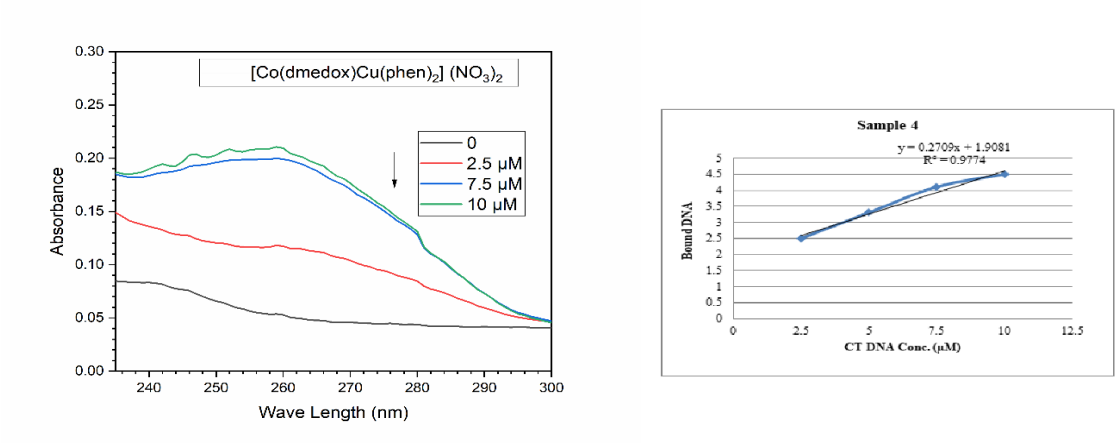

Fig 8: Titration curves of complex **4 by** UV-Visible absorption spectroscopy; buffered (pH = 7.2) at 25 ˚C representing free and fully bound complex.

3.5.2 Deoxyribonucleic acid binding studies by gel electrophoresis

Deoxyribonucleic acid binding assessment of 10 µM test samples of metal complexes **2, 3,** and **4** with their parent ligand **1** with CT-DNA by gel electrophoresis (**Figure 9**) shows that the heterogeneous binuclear complex **4**, with mixed ligands oxamide and 1,10-phenanthroline has 77.72 % highest percentage of binding efficiency compared to its parent ligand dmpdox (**Table 4**). As a result of the structure-activity link, these newly synthesised metal complexes could be useful diagnostic and therapeutic agents in the pharmaceutical industry [50].

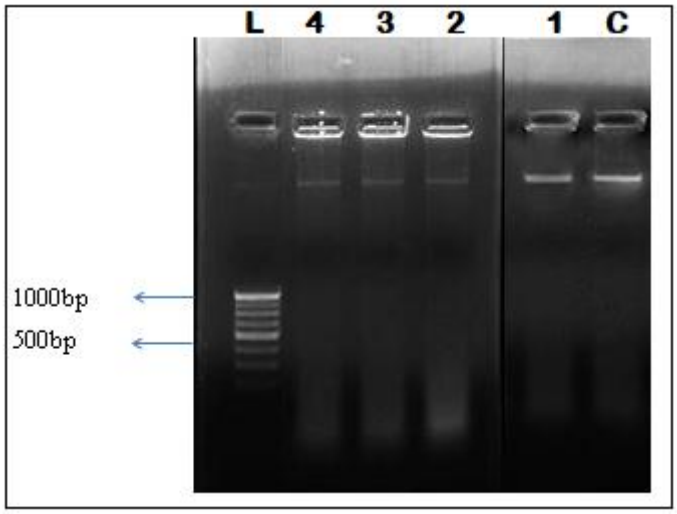

Figure 9: Agarose gel electrophoresis picture displaying binding efficiency of CT-DNA by 10 µM ligand dmpdox **1** and metal complexes **2**, **3** and **4** buffered by 5 mM Tris-HCl and 50 mM sodium chloride, pH = 7.2) at 25 ˚C. where sample 4,3,2 and 1 are loaded in lane 1,2,3 and 4 respectively and L and C are ladder and control respectively.

Table 4: Band intensity and % of binding efficiency of dmpdox **(1)** ligand and its corresponding metal complexes (**2**), (**3**) and (**4**)

Sl. no	Compound	Band intensity (RFU)	Binding Efficiency(%)
(**1**)	Dmpdox (**1**)	10438.14	16.95
(**2**)	[Co (dmpdox) $_2$] (ClO_4) (**2**)	3528.33	71.92
(**3**)	[Co (dmpdox) Co (phen) $_2$] (NO_3) $_2$ (**3**)	3319.43	73.59
(**4**)	[Co (dmpdox) Cu (phen) $_2$] (NO_3) $_2$ (**4**)	2800.36	77.72

[NaCl] = 5 mM; [Tris-HCl] = 50 mM; [Complex] = 10 µM

3.6 Free radical quenching potency

3.6.1 DPPH (2,2-diphenyl-1-picryl-hydrazyl-hydrate) quenching analysis

Metal complexes were tested for DPPH free radical sweeping activity (**Figure 10**) for **1** and monometal complex **2** has shown inhibition lesser than 50% where as both homogeneous and heterogeneous bimetal complexes **3** and **4** has showed notable activity with an IC_{50} value of 26.17 μgmL^{-1} and 24.25 μgmL^{-1}.

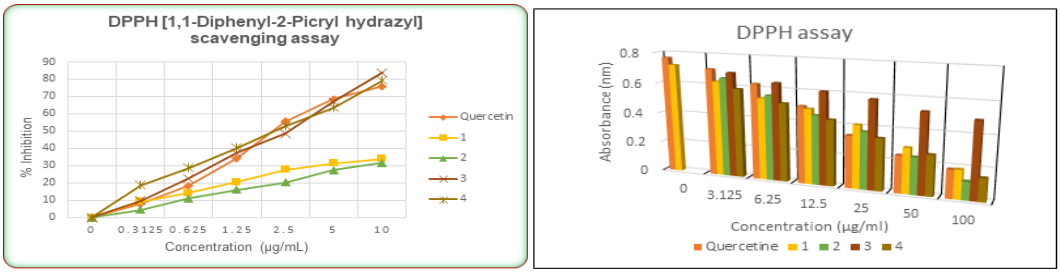

Figure 10: a) Concentration versus % inhibition for DPPH radical scavenging activity compared with positive control quercetin and ligand (**1**) and its metal complexes [Co (dmpdox) $_2$] (ClO_4), (**2**), [Co (dmpdox) Co (phen) $_2$] $(NO_3)_2$ (**3**) and [Co (dmpdox) Cu (phen) $_2$] $(NO_3)_2$ (**4**) b) Bar diagram representing concentration versus absorbance plot of ligand (**1**) ligand and its metal complexes (**2**), (**3**) and (**4**)

3.6.2 Nitric oxide scavenging activity

Mono nuclear metal complex **2**, homo binuclear complex **3** and hetero binuclear metal complex **4** along with ligand **1** treated at 320 μgmL^{-1} exhibited 11.8 µM, 25.5 μgmL^{-1}, 46.8 µM and 278.0 μgmL^{-1} nitric oxide content respectively among the tested complex **4** exhibited moderate nitric oxide scavenging activity (**Figure 11**).

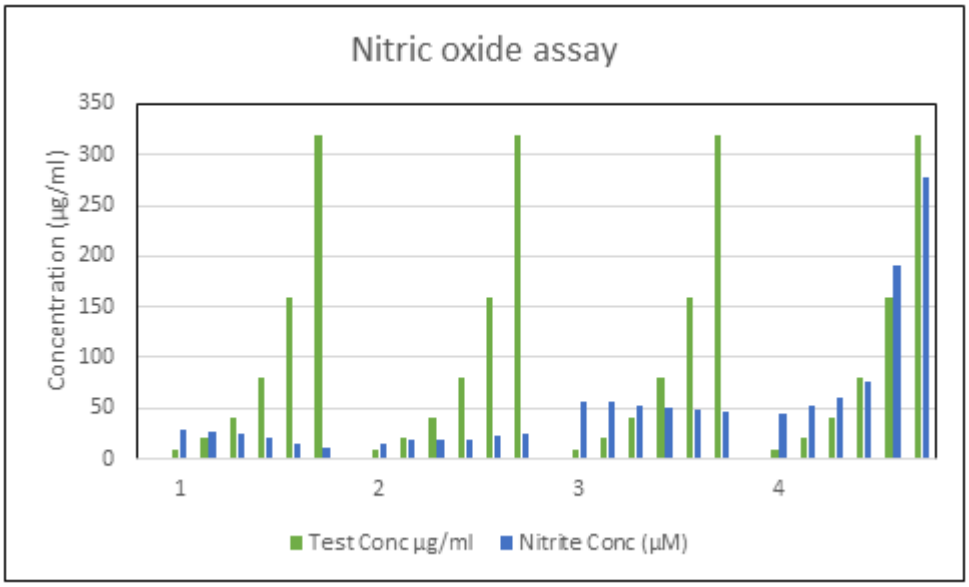

Figure 11: Bar diagram representing concentration of sample versus scavenged concentration of nitrite ion plot of ligand (**1**) and its metal complexes [Co (dmpdox) $_2$] (ClO_4), (**2**), [Co (dmpdox) Co (phen) $_2$] $(NO_3)_2$ (**3**) and [Co (dmpdox) Cu (phen) $_2$] $(NO_3)_2$ (**4**) for nitric oxide radical scavenging activity compared with positive control curcumin.

3.6.3 Superoxide dismutase assay

Mono nuclear metal complex **2**, exhibited 1.72 UmL^{-1} homo binuclear complex **3** exhibited 4.13 UmL^{-1} and hetero binuclear metal complex **4** exhibited 6.15 UmL^{-1} whereas ligand **1** exhibited 1.22 UmL^{-1} with comparison to the parent ligand all the samples exhibited moderate quenching activity against super oxide free radical (**Figure 12**).

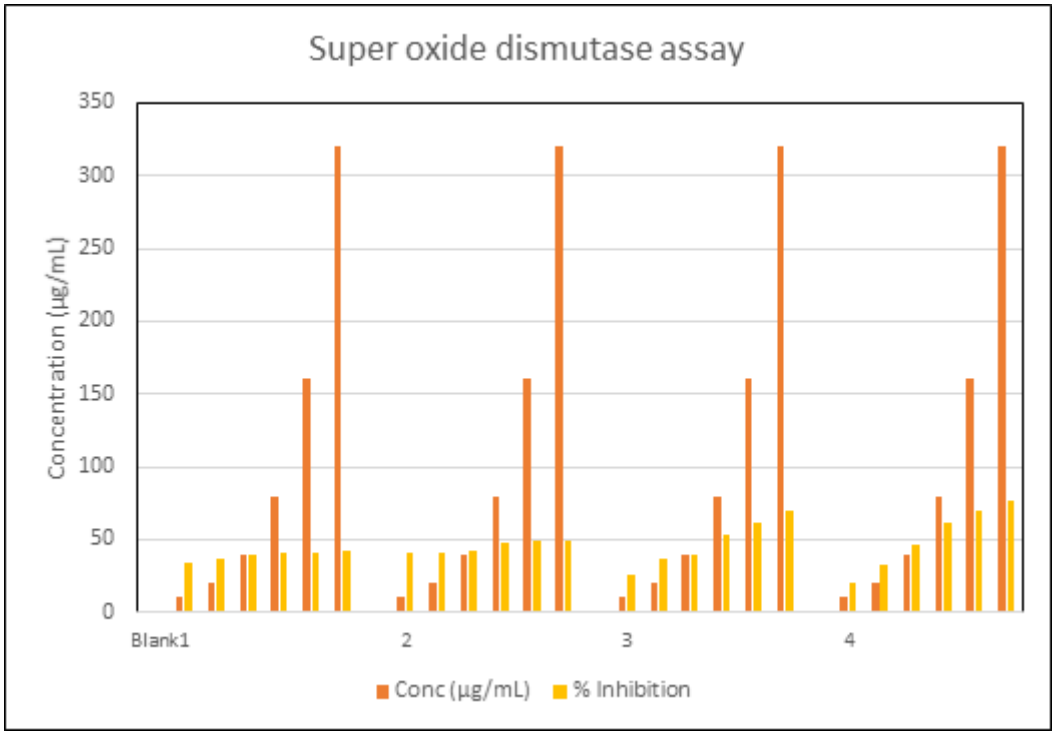

Figure 12: Bar diagram representing concentration of sample versus % inhibition plot of ligand (**1**) and its metal complexes [Co (dmpdox) $_2$] (ClO_4), (**2**), [Co (dmpdox) Co (phen) $_2$] (NO_3) $_2$ (**3**) and [Co (dmpdox) Cu (phen) $_2$] (NO_3) $_2$ (**4**) for nitric oxide radical scavenging activity compared with positive control standard SOD.

3.7 **Cytotoxic activities**

Since all the complexes tested against various cell lines are more carcinogens than the parent ligand. The dose-response curves obtained from nonlinear regression analysis are used to generate the percentage of growth inhibition and test drug oncentration necessary to arrest cell growth by 50% (IC_{50}) are determined using Graph Pad Prism 6 (Figure 13-15). This shows that the coordination of DNA emulation by 1,10-phenanthroline substituted oxamides, which is a recognised DNA intercalating aromatic planar ligand, increases the cytotoxicity of metal complexes. Comparison of IC_{50} values of mononuclear metal complexes with both homo and hetero binuclear complexes in all the cell lines stands evidence for this. The IC_{50} values for mono and bimetal complexes are shown in **Table 5** along with the corresponding ligand**.**

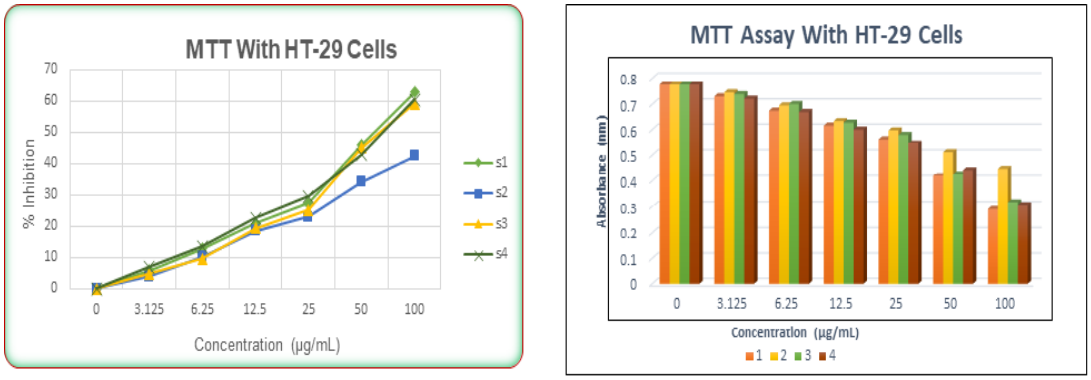

Figure 13: Graphical representation of toxic activity of tested metal complexes versus different concentration of metal Complexes [Co (dmpdox) $_2$] (ClO_4), (**2**), [Co (dmpdox) Co (phen) $_2$] (NO_3) $_2$ (**3**) and [Co (dmpdox) Cu (phen) $_2$] (NO_3) $_2$ (**4**) and its parent ligand (**1**) and Plot exhibiting the relationship between the MTT-measured absorbance and various doses of the ligand dmpdox and its metal complexes against HT-29 cell lines.

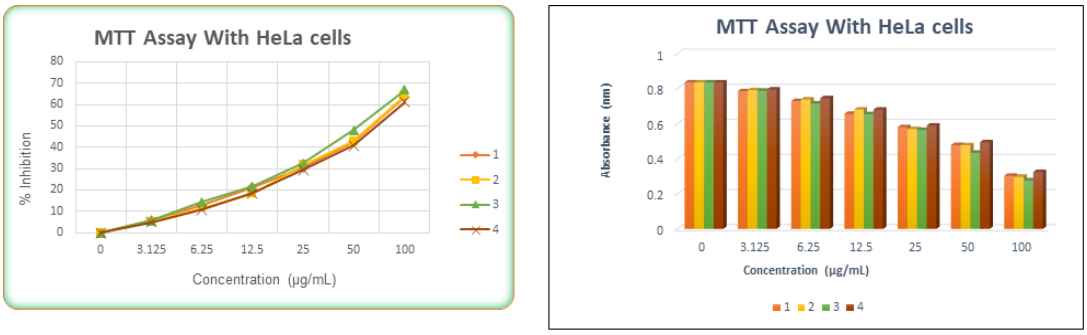

Figure 14: Graphical representation of toxic activity of tested metal complexes versus different concentration of metal complexes [Co (dmpdox) $_2$] (ClO_4), (**2**), [Co (dmpdox) Co (phen) $_2$] (NO_3) $_2$ (**3**) and [Co (dmpdox) Cu (phen) $_2$] (NO_3) $_2$ (**4**) and its parent ligand (**1**) and Plot exhibiting the relationship between the MTT-measured absorbance and various doses of the ligand dmpdox and its metal complexes against HeLa cell lines.

Table 5: Minimum inhibitory concentration of ligand **1** and its **2**, **3** and **4** metal complexes against selected cell lines

Sl. No	**Empirical formula**	**Cancer cell lines**		
		HeLA IC_{50} (μgmL^{-1})	**HT-29 IC_{50} (μgmL^{-1})**	**A549 IC_{50} (μgmL^{-1})**
1	Dmpdox (**1**)	71.42	70.58	-
2	[Co (dmpdox) $_2$] (ClO_4) (**2**)	68.47	-	-
3	[Co (dmpdox) Co (phen) $_2$] (NO_3) $_2$ (**3**)	57.81	60.61	67.13
4	[Co (dmpdox) Cu (phen) $_2$] (NO_3) $_2$ (**4**)	68.97	61.34	72.17

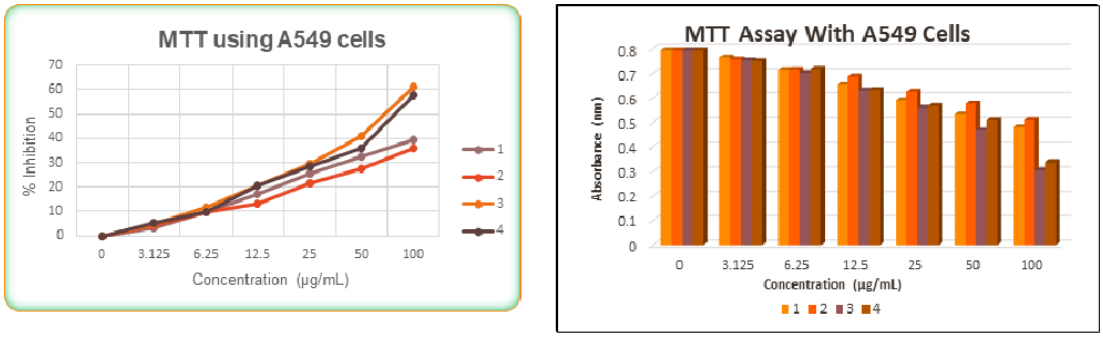

Figure 15: Graphical representation of toxic activity of tested metal complexes versus different concentration of metal complexes [Co (dmpdox) $_2$] (ClO_4), (**2**), [Co (dmpdox) Co (phen) $_2$] (NO_3) $_2$ (**3**) and [Co (dmpdox) Cu (phen) $_2$] (NO_3) $_2$ (**4**) and its parent ligand dmpdox (**1**) and plot exhibiting the relationship between the MTT-measured absorbance and various doses of the ligand dmpdox and its metal complexes with respect to A549 cell lines.

3.8 **Antimicrobial activities**

Bacterium with thick, mesh-like membrane peptidoglycan are termed as gram positive bacterium and bacterium without peptidoglycan are termed as gram negative bacterium. Antibiotic which can inhibit both types of bacteria is a promising agent for medicinal use. All the mononuclear, homobinuclear and hetero binuclear metal complexes were screened for antimicrobial activity (10 mM, 25 µL) (**Figure 16**). It was discovered that complexes **2** and **3** are antagonistic (zone of inhibition was not observed) towards all microorganisms. In contrast, heterogeneous bimetal complex **4** has demonstrated good antibiotic activity (**Table 6**) against both gram positive and gram negative bacterial strains additionally it demonstrated antifungal activity against the fungus Candida albicans, whereas against fungal strains *Aspergillus niger* and *Fusarium oxysporium* antifungal activity was not observed in tested concentration. It is important that the metal complex used as antimicrobial drug must inhibit the cell proliferation at lower drug concentration otherwise it may lead to metal toxicity inside the living system. In this perspective, compared to parent ligand which is negative towards all bacterial and fungal strains complex **4** has exhibited good antimicrobial activity. The collegial effect of oxamide –C=O and N donor atoms of heterocyclic base 1,10-phenanthroline with Co (II) and Cu (II) metal ions influence the antimicrobial activity of metal complex at lower drug concentration

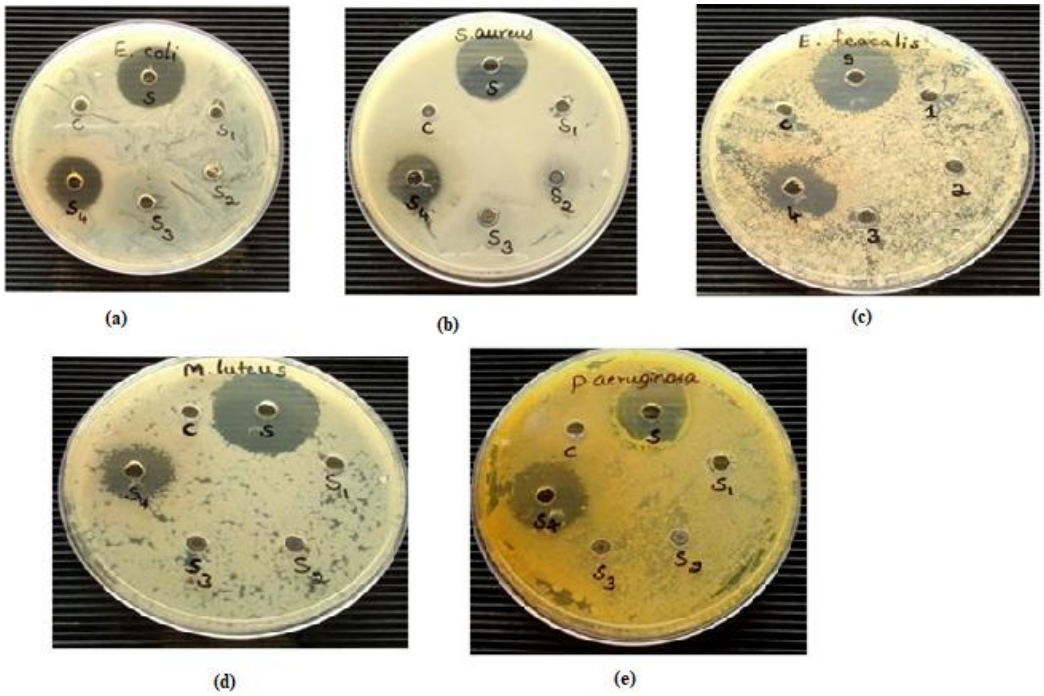

Fig 16: Metal complex **4** induced zone of suppression Of *E. coli* (**a**), *S.aureus* (**b**), *E.feacalis* (**c**) *and M.luteus* (**d**) *;* S-standard (Ciprofloxacin) ; C –Control (DMSO)

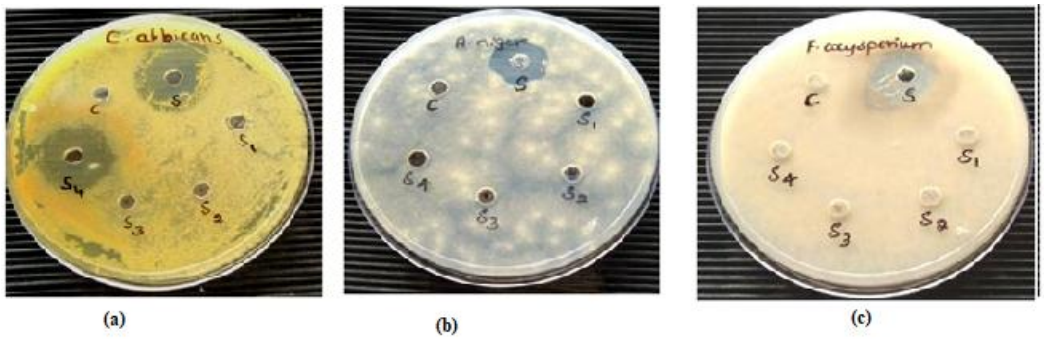

Fig 17: Metal complex **4** induced zone of suppression Of *C.albicans* (**a**), *A.niger*; (**b**) and *F.oxysporium* (**c**) *;* S-standard (Ciprofloxacin) ; C –Control (DMSO)

Table 6: Zone of inhibition induced by complex **4** and its MIC value by micro broth dilution technique using culture medium: Peptone and Potato dextrose broth for respective culture with sample test concentrations 100, 50, 25, 12.5, 6.25, 3.125, 1.56% of against standard ciproflaxin; for bacterial strain and itracanazole; for fungal strains.

Test Organisms	Inhibition zone (mm)	MIC (μgmL^{-1})
E. coli	18±0.0	250
S.aureus	17±0.0	250
E.feacalis	18±0.0	250
M.luteus	20±0.0	125
P.aeruginosa	22±0.0	125
C.albicans	22±0.0	62.5
A.niger	-	-
F.oxysporium	-	-

4. Conclusion

A new mononuclear, homo binuclear and hetero binuclear complexes **[Co (L_1) $_2$]X** (**2**), **[Co (L_1) Co (L) $_2$]X_2** (**3**) and **[Co (L_1) Cu (L) $_2$]X_2** (**4**) were synthesized. ESI-MS, UV-Vis, IR, and NMR spectroscopic analyses were used to characterise new mono complexes. These spectral data provide evidence for the proposed molecular structures of metal complexes **2**, **3**, and **4** as well as confirmation of the coordination of the metal to the ligand. The UV-Vis spectroscopic method was employed to examine the time-dependent stability of all the mono and bimetal complexes revealed that they were stable in the solvent medium, suggesting that biological assays be performed in this reference medium. The carcinogenic activity was studied on human cancer cell lines to evaluate IC_{50} value, all the synthesized complexes exhibited activity towards the tested cell lines. S. aureus, E. feacalis, M. luteus, E. coli, P. aeruginosa, were used to test for antiparasitic activity, and it was discovered that metal complexes **2** and **3** are antagonistic (no zone of inhibition was seen) to all microorganisms. Heterogeneous bimetal complex **4** showed good antibiotic action when tested against bacterial strains of both gram positive and gram negative strains. Whereas, among the *Aspergillus niger* and *Fusarium oxysporium* fungal strains, antifungal activity was not observed in tested concentrations. Antioxidant studies by DPPH free radical quenching assay, nitric oxide assay and superoxide dismutase assay was performed and observed that complex **3** and **4** has showed notable antioxidant activity with an IC_{50} value of 26.17 μgmL^{-1} and 24.25 μgmL^{-1}. Through the use of the electronic absorption spectroscopic technique and the gel electrophoresis, the binding efficiency of the mono and bimetal complexes **2**, **3**, and **4** to CT-DNA was evaluated. The phenanthroline bases in complexes **3** and **4** have expanded planar rings, which promote intercalative mode of binding and non-covalent interactions between the DNA and metal complex that follow the intrinsic binding constants (Kb) of the complexes with CT-DNA in the order **2> 4 > 3**. When compared to its parent ligand **1**, the complex **4** with mixed oxamide and 1,10-phenanthroline ligands has a binding efficiency of 77.72%, according to a gel electrophoresis study. Metal complexes with combinational metal centers augment the possible designing of

therapeutic drugs targeting substrate molecule in a biological system which would be a future scope for medicinal chemistry and clinical pharmacology. As a result of the structure-activity link, these newly synthesised metal complexes could be useful diagnostic and therapeutic agents in the pharmaceutical industry.

5. Conflict of Interest Statement

No conflicts of interest exist, according to the authors.

6. Acknowledgement

One of the authors, Swathi K. R., thanks the UGC for funding her RGNF fellowship so she could carry out this research. A different author, P R Chetana, acknowledges DST for providing her lab with a Gel-Documentation system.

5. References

[1] Raj Kaushal., Sheetal Thakur., Kiran Nehra., 2016, "ct-DNA Binding and Antibacterial Activity of Octahedral Titanium (IV) Heteroleptic (Benzoylacetone and Hydroxamic Acids) Complexes" Int. J. Med. Chem., 2361214, 11 pages.

[2] Alexis C. Komor., Jacqueline K. Barton., 2013, "The path for metal complexes to a DNA target", Chem. Comm. 49, pp. 3605-3614.

[3] Mikhalyova, E A., Kolotilov, S V., Cador, O., Zeller, M., Trofimenko, S., 2012, "The role of the bridging group in exchange coupling in dinuclear homo-and heterometallic Ni (II) and Co (II) complexes with oxalate, oxamidate and dithiooxamidate bridges", Dalton Trans., 41, pp. 11319-29.

[4] Gurumoorthy, P., Mahendiran, D., Prabhu D., Chinnasamy, A., Rahiman, A. K., 2015, "Mixed-ligand copper (II) phenolate complexes: Synthesis, spectral characterization, phosphate-hydrolysis, antioxidant, DNA interaction and cytotoxic studies", J. of Mol. Stru., 1080, pp. 88–98.

[5] Bao-Dui, W., Zheng-Yin, Y., Patrick, C., Da-qi, W., 2007, "Synthesis, crystal structure and DNA-binding studies of the Ln (III) complex with 6-hydroxychromone-3-carbaldehyde benzoyl hydrazone", J. of Inorg. Biochem. 101, pp 1492–1504.

[6] Xin, Li., Yan-Tuan, Li., Zhi-Yong, W., Yong-Jun, Z, Cui-Wei, Y., 2012, "Synthesis, structure, DNA-binding properties and cytotoxic activities of a new one-dimensional polymeric copper (II) complex with N-benzoate-N'-[3-(2-hydroxyl-ethylammino) propyl] oxamide as ligand", *Inorganica Chimica Acta*., 385 150–157.

[7] Qi-Hua Zhao., Xiao-Feng Wang., Rui-Bin., 2005, "Two novel oxamido-bridge dinuclear copper (II) complexes containing four spin carriers involving the nitroxide radical ligand: synthesis, crystal structure and magnetic properties", Trans. Met. Chem., 30, pp. 527–531.

[8] Yves Journaux., Jorunn Sletten., Olivier Kahn., 1985, "Tunable interaction in μ-oxamido copper (II) binuclear complexes", Inorg. Chem., 24, pp. 4063-4069.

[9] Hong-Hua, L., Yan-Tuan, L., Zhi-Yong, W., Kang Zheng., Cui-Wei, Y., 2011, "Synthesis, structure, and DNA-binding studies of a dicopper (II) complex with N-phenolato-N′-[2-(dimethylamino) ethyl]oxamide as ligand", J. Coord. Chem., 64 (8), pp. 1360–1374.

[10] Mikhalyova, E A., Kolotilov, S V., Cador, O., Zeller, M., Trofimenko, S., 2012, "The role of the bridging group in exchange coupling in dinuclear homo-and heterometallic Ni (II) and Co (II) complexes with oxalate, oxamidate and dithiooxamidate bridges", Dalton Trans., 41, pp. 11319-29.

[11] Aliasghar, J., Khalili, D., Erik De Clercq., Salmi, Chanaz., Brunel, J M., 2007, "Synthesis, Antibacterial, Antifungal and Antiviral Activity Evaluation of Some New bis-Schiff Bases of Isatin and Their Derivatives", Molecules., 12 (8), pp. 1720-1730.

[12] Jan, M., Maria, G-A., Maria, P., Martin, L., Milan, z. Rivas-Gonzalo, J. C., 2007, "Measurement of Antioxidant Activity of Wine Catechins, Procyanidins, Anthocyanins and Pyranoanthocyanins", Int. J. Mol. Sci., 8 (8), pp. 797-809.

[13] Nishat, N., Rahisuddin., Haq, M. M., Vikrant Kumar., 2006, "Synthesis, characterization and antimicrobial activity studies of N-N ′-tetracarboxydiethyloxamide ligand and its metal (II) complexes", J. Coord. Chem., 59 (15), pp. 1729–1738.

[14] Pragnesh, K.P., Parekh, M. H., Pansuriya, B. P., Mohan, N. P., 2006, "Bactericidal activity of different oxovanadium (IV) complexes with Schiff bases and application of chelation theory", J. Enzyme Inhibition and Med. Chem., 21 (2), pp. 203–209.

[15] Feng-Jia, Z., Hong Qin, Fang Liu, Y. L., Tuan, Zhi W., Yong, Y., Cui-Wei., 2015, "Synthesis and crystal structure of new dicopper (II) complexes with N,N'-bis-(dipropylenetriamine) oxamide as bridging ligand: Effects of the counterions on DNA/protein-binding property and in vitro antitumor activity", J. Photochem. and Photobiology: B Biology. 143, pp. 148-162

[16] Yan-Tuan Lia., Qiang-Ming, W., Cui-Wei, Y., Chun-Yuan., 2004, "Synthesis and magnetic properties of copper (II) –lanthanide (III) heterobinuclear complexes with N,N'-bis[3-(dimethylamino) propyl]oxamido as ligand", J. Magnetism and Magnetic Materials., 283, pp. 215–222.

[17] Xiao-Wen, L., Man Jiangy, L., Yan-Tuan, Zhi-Yong, W., Cui-Wei Yan., 2010, "Synthesis, structure, and DNA-binding studies of a new tetracopper (II) complex bridged by dissymmetrical N-benzoato-N'-(2-aminoethyl) oxamide", J Coord. Chem, 63 (9), pp. 1582–1596.

[18] Chen, W. C., Wang, L. D., Yan-Tuan, L., Zhi-Yong, W., Cui-Wei, Y., 2012, "Synthesis, crystal structure, cytotoxicities and DNA-binding properties of a tetracopper (II) complex with N-benzoato-N'-[2-(2-hydroxyethylamino) ethyl-amino]oxamide ligand", Transition Met Chem., 37, pp. 569–577.

[19] Laila, H., Abdel-Rahman, El-Khatib Rafat, M., Nassr Lobna, A.E., Abu-Dief Ahmed, M., Mohamed Ismael, Amin Abdou Seleem., 2014, "Metal based pharmacologically active agents: Synthesis, structural characterization, molecular

modeling, CT-DNA binding studies and in vitro antimicrobial screening of iron (II) bromosalicylidene amino acid chelates", Spectrochimica Acta., 117, pp. 366–378.

[20] Ramana, N., Sobha, S., Thamaraichelvan, A., 2011, "A novel bioactive tyramine derived Schiff base and its transition metal complexes as selective DNA binding agents", *Spectrochimica Acta*., 78, pp. 888–898.

[21] Liang Ningjian, D. Kitts David., 2014, "Antioxidant Property of Coffee Components: Assessment of Methods that Define Mechanisms of Action", Molecules, 19, pp. 19180-19208.

[22] Ekennia Anthony, C., Osowole Aderoju, A., Olasunkanmi Lukman, O., Onwudiwe Damian, C., Eno, E., 2017, **"**Coordination behaviours of new (bidentate N,O chelating) Schiff bases towards copper (II) and nickel (II) metal ions: synthesis, characterization, antimicrobial, antioxidant, and DFT studies**",** Research Chem. Intermed., 43, pp 3787–3811.

[23] Fei Xue., Cheng-Zhi Xie., Yan-Wen Zhang., Zheng Qia., Xin Qiao., Jing-Yuan., Shi-Ping, Y., 2012, "Two new dicopper (II) complexes with oxamido-bridged ligand: Synthesis, crystal structures, DNA binding/cleavage and BSA binding activity", J. Inorg. Biochem. 115, pp. 78–86.

[24] Amy M. B., Seth M. C., M. H. Lim., K., 2013, "Medicinal inorganic chemistry: a web themed issue", ***Chem. Commun.***, **49**, pp. 5910-5911.

[25] Gonzalez, R.J., Tarloff, J.B., 2001, "Evaluation of hepatic subcellular fractions for alamar blue and MTT reductase activity", *Toxicology in Vitro*., 15, pp. 257–259.

[26] Hattori, N., Sakakibara, T., Kajiyama, N., Igarashi, T., Maeda, M., Murakami, S., 2003, "Enhanced microbial biomass assay using mutant luciferase resistant to benzalkonium chloride", *Anal. Biochem.*, 319, pp. 287-295.

[27] Lundin, A., Hasenson M., Pearson, J., Pousette, A., 1983, "Estimation of Biomass in Growing Cell Lines by Adenosine Triphosphate Assay", Methods in enzymol., 133, pp. 27-42.

[28] Francois, D.; Rita, L., 1986, "Rapid colorimetric assay for cell growth and survival Modifications to the tetrazolium dye procedure giving improved sensitivity and reliability", J. Immunological Methods., 89, pp. 271-272.

[29] Jahangiriana, H., Md Jelas Haronb, Mohd Halim S., Ismail, A., Rafiee-Moghaddamc, R., Leili Afsah-Hejri., Yadollah Abdollahi, E., Majid Rezayi, C., Nazanin Vafaei, F. Digest., 2013, "Well diffusion method for evaluation of antibacterial activity of copper phenyl fatty hydroxamate synthesized from canola and palm kernel oils", J. Nanomaterials and Biostructures., 8 (3), pp. 1263-1270.

[30] Ahamad, T., Kumar, V., Parveen, S., Nishat, N., 2008, "Synthesis, characterization and antimicrobial activity of poly (ethylene oxamide-N,N ′-disuccinate) and its polymer metal complexes", J. Coord. Chem., 61 (9), 1423-436.

[31] Jia-qing Xie.; Bing-ying, J.; Xing-ming, K.; Chang-wei, H.; Xian-cheng, Z., **2003**, "Studies on the reaction kinetics and the mechanism of hydrolysis of bis (4-nitrophenyl) phosphate (BNPP) catalyzed by oxamido-bridged dinuclear copper (II) complexes in micellar solution", Trans. Met. Chem., 28, pp. 782-787.

[32] Fang-Hong He., Lin Tao., Xiao-Wen, L., Yan-Tuan, L., Zhi-Yong, W., Cui-Wei, Y., 2012, "Syntheses and structures of new dicopper (II) complexes bridged by N-(2-hydroxyphenyl)-N'-(3-aminopropyl) oxamide: DNA-binding properties and cytotoxic activities", New J. Chem., pp. 2078-2087.

[33] Ajaykumar, K., Patil Sangamesh, A., Prema, S, B., 2009, "Synthesis, characterization, DNA cleavage and in vitro antimicrobial studies of La (III), Th (IV) and VO (IV) complexes with Schiff bases of coumarin derivatives", Euro. J. Med. Chem., 44 (7), pp. 2904-2912.

[34] Xiao-Wen, L., Yan-Tuan, L., Zhi-Yong, W., Cui-Wei, Y., 2012, "Syntheses and structures of bicopper (II) complexes bridged by N-(5-chloro-2-hydroxyphenyl)-N'-[3-(dimethylamino) propyl] oxamide: Cytotoxic activities, and reactivities towards DNA and protein", Inorganica Chimica Acta., 390, pp. 190-198.

[35] Xiao-Wen, L., Yong-Jun Zheng., Yan-Tuan, L., Zhi-Yong, W., Cui-Wei, Y., 2011, "Synthesis and structure of new bicopper (II) complexes bridged by N-(2-aminopropyl)-N'-(2-oxidophenyl) oxamide: The effects of terminal ligands on structures, anticancer activities and DNA-binding properties", Euro. J. Med. Chem., 46 (9), pp. 3851-3857.

[36] Avaji Prakash, G., Patil Sangamesh, A., 2007, "Synthesis, spectral, thermal, solid state d.c. electrical conductivity and biological studies of lanthanum (III) and thorium (IV) complexes with thiocarbohydrazone", Trans. Met. Chem., 32, pp. 379-386.

[37] Avaji Prakash, G., Nagaraja, B. R., Patil., Sangamesh, A., 2006, "Synthesis, spectral characterization, biological and fluorescence studies of lanthanum (III) complexes with 3-substituted-4-amino-5-hydrazino-1,2,4-triazole Schiff bases", Trans. Met. Chem., 31, pp. 842-848.

[38] Mrkalic Emina, M., Jelic Ratomir, M., Klisuric Olivera, R., Matovic Zoran, D., 2014, "Synthesis of novel palladium (II) complexes with oxalic acid diamide derivatives and their interaction with nucleosides and proteins. Structural, solution, and computational study", Dalton Trans., 43, pp. 15126-15137.

[39] Casellato., Guerriero, P., Tamburini, S., Vigato, P.A., 1997, "Metal complexes with disubstituted oxamidic ligands", Inorganica Chimica Acta., 260 (1), 1-9.

[40] Siddappa, K., Mane Sunilkumar, B., Manikprabhu, D., 2014, "La (III) complex involving the O, N-donor environment of quinazoline-4 (3H)-one Schiff's base and their antimicrobial attributes against methicillin-resistant Staphylococcus aureus (MRSA) ", Spectrochimica Acta, Part A: Mol. and Biomol. Spect, 130, pp. 634-638.

[41] Beeston Ruth, F., Stephen Aldridge, W., Treadway Joseph, A., Fitzgerald Michael, C., DeGraff Benjamin, A., Stitze Shannon, E., 1998, "Synthesis, Characterization, and Photochemical/Photophysical Properties of Ruthenium (II) Complexes with Hexadentate Bipyridine and Phenanthroline Ligands", Inorg. Chem., 37, pp. 4368-4379.

[42] Chetana, P. R., Ramakrishna, R., Saha, S., Policegoudra, R. S., Vijayan, P., Aradhya, M. S., 2012, "Oxidative DNA cleavage, cytotoxicity and antimicrobial studies of L-ornithine copper (II) complexes", *Polyhedron*., 43-50.

[43] Xiao-Wen, L., Lin Tao., Yan-Tuan, L., Zhi-Yong, W., Cui-Wei, Y., 2012, "Bimetallic complexes constructed from asymmetrical N,N'-bis (substituted)-oxamide: Cytotoxicities, and reactivities towards DNA and protein", Euro. J. Med. Chem., 54, pp. 697-708.

[44] Cui-Wei, Y., Yan-Tuan, L., Dai-Zheng Liao., 1997, "Synthesis and magnetic properties of heterobinuclear copper (II) iron (II) complexes with N.N'-bis (2-aminopropyl) oxamidocopper (II) ", Trans. Met. Chem., 22, pp. 475-478

[45] Yan Tuan, L., Cui Wei, Y., Chun Yuan, Z., Hua Shi Guan., 2004, "Synthesis and Magnetic Studies of μ-Oxamido-bridged Copper (II) Manganese (II) Heterobinuclear Complexes" Syn. and Reac. Inorg. and Met. Org. Chem., 34 (7), pp. 1165-1179.

[46] Arnold, S., Gitta, S., 2019, "An Organic Chemist's Guide to Electrospray Mass Spectrometric Structure Elucidation", Molecules., 24, pp. 611.

[47] Konermann, L., Ahadi, E., Rodriguez Antony, D., Vahidi, S., 2013, "Unraveling the Mechanism of Electrospray Ionization", Anal. Chem., 85, pp. 2-9.

[48] Tian-Rong, L., Zheng-Yin Yang., Bao-Dui Wang., Dong-Dong Qin., 2008, "Synthesis, characterization, antioxidant activity and DNA-binding studies of two rare earth (III) complexes with naringenin-2-hydroxy benzoyl hydrazone ligand", Euro. J. Med. Chem., 43 (8), pp. 1688-1695.

[49] Shi-Hao, C., Man Jiang, Yan-Tuan, Li., Zhi-Yong, W., Xiao, Wen, Li., 2011, "Synthesis, structure, DNA-binding, and cytotoxic activities of N-(5-chloro-2-hydroxyphenyl)-N′-[3-(2-hydroxyethylamino) propyl]oxamide and its dicopper (II) complex", Journal of Coordination Chemistry., 64 (23), pp. 4209–4224.

[50] Mahmood Dar, A., Ishrat, U.; Yaseen, Z., Shamsuzzaman., Ahmad Gatoo, M. J., 2015, "In vitro cytotoxcity and interaction of new steroidal oxadiazinanones with calf thymus DNA using molecular docking, gel electrophoresis and spectroscopic techniques", Photochem., Photobio.: Biology, 148, pp. 340-350.

[51] Qian-Ling Zhang., Jin-Gang Liu., Hui Chao., Gen-Qiang Xue., Liang-Nian Ji., 2001, "DNA-binding and photocleavage studies of cobalt (III) polypyridyl complexes", J. Inorg. Biochem., 83 (1), pp. 49-55.